Since January 2020 Elsevier has created a COVID-19 resource centre with free information in English and Mandarin on the novel coronavirus COVID-19. The COVID-19 resource centre is hosted on Elsevier Connect, the company's public news and information website.

Sensors & Actuators: B. Chemical 362 (2022) 131764

Contents lists available at ScienceDirect

Sensors and Actuators: B. Chemical

journal homepage: www.elsevier.com/locate/snb

Prospects of NIR fluorescent nanosensors for green detection of SARS-CoV-2

Dan Li [a,*], Zipeng Zhou [b], Jiachen Sun [b], Xifan Mei [b,*]

[a] Department of Basic Science, Jinzhou Medical University, 40 Songpo Road, Jinzhou 121001, China
[b] Department of Key Laboratory of Medical Tissue Engineering of Liaoning, Jinzhou Medical University, 40 Songpo Road, Jinzhou 121001, China

ARTICLE INFO

Keywords:
SARS-CoV-2
NIR
Nanosensor
Green synthesis
Environmental-friendly
Low-toxic

ABSTRACT

The pandemic of the novel coronavirus disease 2019 (COVID-19) is continuously causing hazards for the world. Effective detection of severe acute respiratory syndrome coronavirus 2 (SARS-CoV-2) can relieve the impact, but various toxic chemicals are also released into the environment. Fluorescence sensors offer a facile analytical strategy. During fluorescence sensing, biological samples such as tissues and body fluids have autofluorescence, giving false-positive/negative results because of the interferences. Fluorescence near-infrared (NIR) nanosensors can be designed from low-toxic materials with insignificant background signals. Although this research is still in its infancy, further developments in this field have the potential for sustainable detection of SARS-CoV-2. Herein, we summarize the reported NIR fluorescent nanosensors with the potential to detect SARS-CoV-2. The green synthesis of NIR fluorescent nanomaterials, environmentally compatible sensing strategies, and possible methods to reduce the testing frequencies are discussed. Further optimization strategies for developing NIR fluorescent nanosensors to facilitate greener diagnostics of SARS-CoV-2 for pandemic control are proposed.

1. Introduction

Severe acute respiratory syndrome coronavirus 2 (SARS-CoV-2) is the virus causing the respiratory illness of the novel coronavirus disease 2019 (COVID-19).[1] This virus can damage various organs including the lung, [2] heart, [3] kidney, [4] and brain, [5] which even cause long-term health problems after cure. [6] Effective analysis of SARS-CoV-2 can relieve the damage of COVID-19. [7–9] Various methods including molecular (such as ribonucleic acid (RNA)), [7,10, 11] antigen, [12–14] or antibody [15–17] tests have been developed for monitoring SARS-CoV-2 infections. [18] Especially, thanks to the gold standard Polymerase Chain Reaction (PCR) facilities, the burden for the

List of abbreviations: SARS-CoV-2, Severe acute respiratory syndrome coronavirus; COVID-19, The pandemic of the novel coronavirus disease 2019; NIR, Near-Infrared; PCR, Polymerase Chain Reaction; RNA, ribonucleic acid; POC, point-of-care; RCA, rolling circle amplification; DPV, Differential pulse voltammetry; VIS, visible; IgG, immunoglobulin G; IgM, immunoglobulin M; SWCNTs, single-walled carbon nanotubes; IgG A, IgG aggregation; NIR775, an H_2S-inert fluorophore; Cy7Cl, a cationic cyanine dye; FRET, fluorescence resonance energy transfer; IONPs, iron oxide nanoparticles.; P, FITC-labelled GzmB substrate peptides; LICOR, IRDye-800CW; EB-NS, prepared by the layered pigment CaCuSi4O10 (Egyptian Blue, EB) via ball milling and facile tip sonication into NIR fluorescent nanosheets; DSNP, down shifting nanoparticles; DSNP@MY-1057-GPC-3, active targeting antibody glypican-3 (GPC-3) was conjugated with DSNP@MY-1057; HCC, hepatocellular carcinoma; Pb-Ag_2S ODs, lead doped Ag_2S quantum dots; SPNs., semiconducting polymer nanoparticles; R, R represents a common recognition element for the target; HA1, hemagglutinin subunit.; HAS, serum albumin; N protein, nucleocapsid protein; S protein, spike protein; ACE2, Angiotensin-converting enzyme 2; S RBD, SARS-CoV-2 spike receptor-binding domain; MERS, Middle East respiratory syndrome coronavirus; HA1., hemagglutinin subunit; VTM, viral transport medium; pGOLD, plasmonic gold; AIE, aggregation-induced emission; PS, polystyrene; LED, light emitting diode; MCU, microcontroller unit; CdS, core/shell lead sulfide/cadmium sulfide; QDs, quantum dots; PEG, branched by Polyethylene glycol; PEG1000 PE, 1,2-distearoyl-sn-glycero-3-phosphoethanolamine-N-[methoxy(polyethylene glycol)– 1000]; PEG2000 PE, (1,2-distearoyl-sn-glycero-3-phosphoethanolamine-N-[methoxy(polyethylene glycol)– 2000);; CF647, a cyanine-based far-red fluorescent dye; CP-MNB, capture probe-conjugated magnetic bead particle; E, envelope; S, spike; M, membrane; N, nucleocapsid; Si-RP, silica-reporter probe; SPNs, semiconducting polymer nanoparticles.; IONPs., iron oxide nanoparticles; ASOs, antisense oligonucleotides; FLU, an infectious disease caused by influenza viruses; SAM, self-assembled monolayer; PBS, Phosphate-buffered saline; CoPhMoRe, corona phase molecular recognition; $AIE_{810}NP$, an aggregation-induced emission (AIE) nanoparticle (λ_{em} = 810 nm); 5 G, the fifth generation technology standard for broadband cellular networks; DCNPs, Down-conversion nanoparticles; AIEgens, AIE luminogens; ENMs, electrospun nanofibrous membranes; AuNP, Gold nanoparticle; QY, quantum yield.

* Corresponding authors.
E-mail addresses: danli@jzmu.edu.cn (D. Li), meixifan@jzmu.edu.cn (X. Mei).

https://doi.org/10.1016/j.snb.2022.131764
Received 3 November 2021; Received in revised form 22 February 2022; Accepted 21 March 2022
Available online 30 March 2022

spread of the infections is significantly relieved based on the detection of SARS-CoV-2 RNA. [19–21].

The virus genome of SARS-CoV-2 is a single positive-stranded RNA of about 30,000 bases, which contains genes including replicas complex (*orf1ab*), the 5′ untranslated region, envelope *(E)*, spike *(S)*, membrane *(M)*, nucleocapsid *(N)* structural proteins, 3′-untranslated region, and several unidentified non-structural open reading frames. [22,23] The molecular tests have been developed to detect one or several of these genes to recognize the virus. For instance, a setup that involved step-wise sandwich hybridization of rolling circle amplification (RCA) amplicons with electrochemical sensors (Fig. 1) was designed. [24] This sandwich was constructed by the capture probe-conjugated magnetic bead particle (CP-MNB), the target, and the silica-reporter probe (Si-RP), which were mixed in a single hybridization step and subsequently a single washing step. Differential pulse voltammetry (DPV) showed enhanced signals while interacting with the viral N or S genes of SARS-CoV-2 with a detection limit of 1 copy/μL. This method accurately evaluates 106 clinical samples through a simplified protocol compared

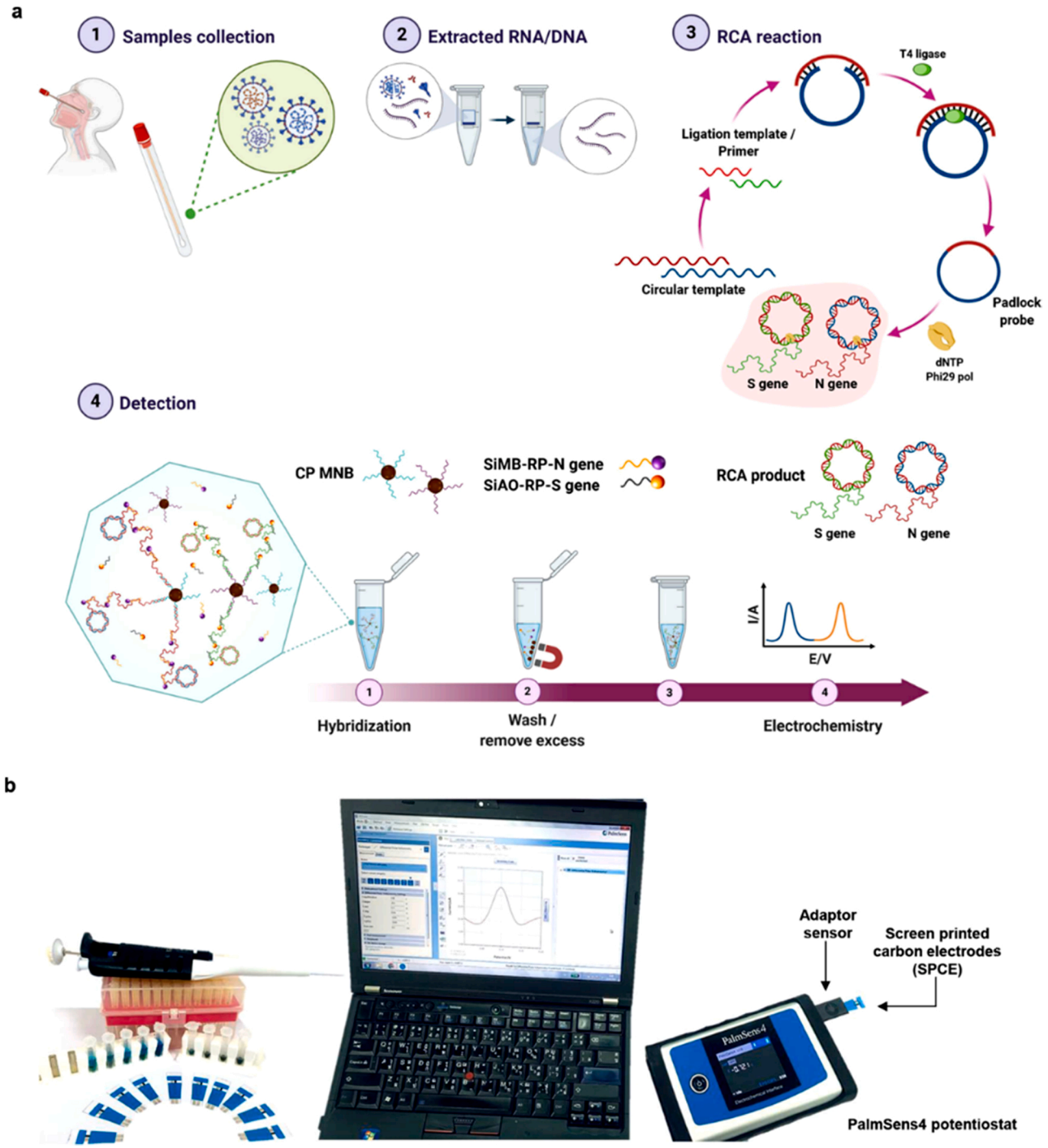

Fig. 1. a, a scheme for the extraction and analysis of SARS-CoV-2 RNA from clinical samples using the electrochemical biosensors with RCA of the N and S genes. b, The electrochemical analysis by using a portable potentiostat device connected to a laptop. Note: The N gene is the nucleocapsid protein for RNA packaging and viral particle release.
Reprinted from ref.[24] with permission from Springer Nature (copyright 2021).

to many methods that minimize contamination to optimized values. However, the viral RNA has to be extracted for SARS-CoV-2 analysis, which is required by most current techniques. [25–27] During the extraction processes, necessary toxic RNA isolation reagents are needed. [28–31] To better protect the environment, finding strategies to reduce the release of toxic substances becomes the need for new strategies.

Outbreaks occur from time to time, but some methods may not be sensitive or accurate enough. [32–35] Many diagnostic tests can give false positive or negative results for complex reasons. [36,37] Then, multiple repeat tests may be needed to confirm the positive or negative cases. A sensitive test can not stop the frequent use of test kits because diagnosis is mostly not dynamic. For instance, a patient's viral infection status may fluctuate between negative and positive. [38] This necessitates an increase in the test frequency. Increased test frequency results in more waste being generated. Therefore, flexible strategies to adapt to dynamic viral infections may reduce the test frequency and the disposable test kits.

Nanomaterial-based biosensors require affordable equipment and simple operating procedures. These biosensors are promising to reduce environmental hazards from synthesis to recycling. [39–41] For instance, some nanomaterials-based biosensors match the accuracy, sensitivity, and specificity for an RNA-extraction-free nano-amplified test of SARS-CoV-2 using color readout. [42,43] Compared to the color sensor, some fluorescence detection can be more sensitive without using the amplification or extraction processes. [44–46] This may significantly reduce the waste generated during analysis progresses.

The traditional fluorescent sensor detects analytes from ultraviolet (UV) to visible (VIS) emission, but the signal at this UV–VIS range may suffer interferences from the biological samples (e. g., the proteins in the serum have green fluorescence). [47,48] On the other hand, biological samples have ultra-low NIR (NIR I (ca. 700–1100 nm), NIR-II (1000–1700 nm) fluorescence signals. [49–52] Then, the NIR fluorescent nanosensors may more accurately diagnose COVID-19 suffering fewer interferences (Fig. 2), providing a promising platform to reduce the misdiagnosis results. This will even reduce additional confirmed tests.

Some NIR fluorescent nanosensors show potential from raw material production to waste recycling. NIR fluorescent nanosensors can be designed through green methods and low-toxic NIR fluorescent nanomaterials; [53] It can also be fabricated based on the loading of NIR organic dyes on low-toxic but non-fluorescent nanomaterials (Table 1). In combination with a bioreceptor (or biological recognition element), the analytes could be detected by reading the NIR emissions with an appropriate excitation. [54].

Though the reported NIR fluorescent nanosensors of SARS-CoV-2 detections are limited, several reports have already shown promise for both accurate and environmental-friendly analysis, which covers the detection of SARS-CoV-2 RNA, the recognition of the antigen of this virus, and the antibody test such as the analysis of human immunoglobulin G (IgG), immunoglobulin M (IgM), and IgG avidity at different infection stages. However, the hazard release during the life cycle of the NIR fluorescent sensing is still expected to be modified for better environmental protection. [66,67] Herein, we focused on presenting these reported NIR fluorescent nanosensors for the potential detection of SARS-CoV-2. To reduce long-term pollution, the green synthesis, detection, and recovery for analysis of SARS-CoV-2 based on NIR fluorescent sensors are discussed. The prospects toward designing more environmental-friendly tests using NIR fluorescent nanosensing methods are proposed for the sustainable diagnosis of COVID-19.

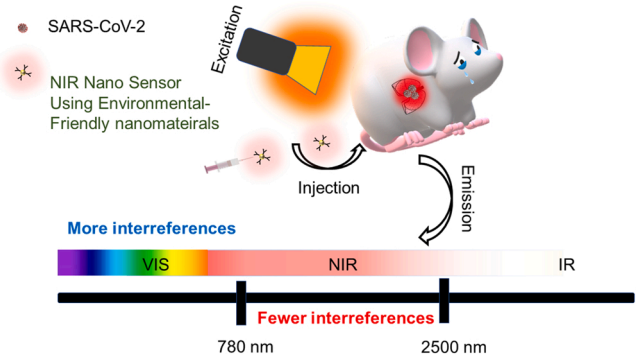

Fig. 2. A promising platform for in-vivo sensing of SARS-CoV-2 using NIR fluorescent nanosensor based on the employment of NIR fluorescent nanomaterials with environmental-friendly properties.

2. Molecular test

Molecular tests based on NIR fluorescent nanosensors detect genetic material - the RNA - of the SARS-CoV-2. [68] For instance, antisense oligonucleotides (ASOs) are single-stranded oligodeoxynucleotides that can be used as a bioreceptor to target the viral RNA. [69] Moitra et al. employed ASOs (50-CCAATGTGATCTTTTGGTGT-30) to conjugate NIR-II fluorescent lead sulfide quantum dot (PbS QD) using a UV-triggered thiol–ene (also called alkene hydrothiolation) click chemistry (Fig. 3a). The developed sensor (PbS QD-ASO) exhibits aggregation-induced NIR-II emission specifically in the presence of RNA (Fig. 3b-d) extracted from clinical SARS-CoV-2 positive samples. The deep tissue penetration ability of NIR fluorescence (2–4 mm at 900–1900 nm) enabled the ex-vivo imaging (ca. 1000 nm) of the infected lungs of BALB/c (BALB/c is an albino, which refers to the immunodeficient laboratory-bred strain of the house mouse) mouse model, showing excellent specificity due to the hybridization of the ASOs (from PbS QD-ASO) with the viral RNA strands. PbS QDs are semiconductors, which are popular for NIR fluorescent sensing applications due to their simple synthesis process, excellent light absorption performance, low cost, and tunable band gap. [70] Though the involvement of the toxic metal (Pb) from PbS QD may be a concern, it was reported that PbS QD protected by an inner layer such as polyethylene glycol (PEG) exhibited high aqueous stability, biocompatibility and remained highly fluorescent for noninvasive, fast, real-time bioimaging. [71] The confinement of NIR fluorescent QDs by inner polymers may be an effective way to reduce the release of the toxic Pb. However, stable PbS QDs were mostly stabilized by a capped ligand, which was not soluble in water. For instance, oleic acid capped PbS QD requires phase transfer before biomedical applications. [72] In addition, to modify the bioreceptor (ASO) on PbS QD for imaging of SARS-CoV-2 infected samples, UV-induced thiol-ene click chemistry was used, which also required an organic chemical pollutant (dimethoxypropiophenone (DMPA)). Similar to most tests, RNA extraction was a necessary procedure when the sensitivity could not meet the extraction-free analysis. Thus, further modifications of PbS QD-based sensors for more environmentally-friendly discrimination of SARS-CoV-2 infected samples are still expected.

3. Antigen test

3.1. Enzyme receptor

In the reported works, COVID-19 antigen tests mainly depend on the detection of the nucleocapsid protein (N protein) or spike protein (S protein) of SARS-CoV-2. [73] Bioreceptors are normally attached to the NIR fluorescent materials in these sensors for recognizing the antigens. Angiotensin-converting enzyme 2 (ACE2) is an enzyme that can attach to the membrane of cells (mACE2) in the intestines, testis, kidney, gallbladder, and heart. [74] ACE2 can be used as a bioreceptor to non-covalently bind to S protein with high affinity. [75] Pinals et al. employed ACE2 as a bioreceptor for functionalization of NIR fluorescent SWCNTs, which could target recombinant coronavirus S protein. Excited at 721 nm, the sensor showed brighter NIR fluorescence (1130 nm)

Table 1
Examples of the NIR fluorescent nanosensors for the detection of various analytes.

Sensors	Chromophores	Main hazard release	Analysis target	Readout	Ref.
SWCNTs-R	SWCNTs	The organic reagents during the production	Bacteria; Serotonin; H_2O_2; IgG A; Cytometry; metal ions, etc.	900–1250 nm	[55–59]
EB-NS-R	EB-NS	The release of Cu^{2+}	Potential bioimaging for various analytes	910 nm	[60]
Pb-Ag_2S ODs-R	Pb-Ag_2S ODs	The release of Pb^{2+}	H_2O_2	1200 nm	[61]
SPNs-R	SPNs	The ogrianic reagents during the production	Cancer	1300–1400 nm	[62]
IONPs-P-LICOR	*LICOR*	*The release of organic dyes*	*GzmB activity*	*about 800 nm*	[63]
NIR775/ Cy7Cl@HyNPs	*NIR775, Cy7Cl*	*The release of organic dyes*	*H_2S*	*775–810 nm (FRET)*	[64]
DSNP@MY-1057-GPC-3	*MY-1057*	*The release of organic dyes*	*HCC*	*1060 nm*	[65]

SWCNTs, single-walled carbon nanotubes; SWCNTs-R, SWCNTs in combination with a receptor (R); R in sensors represent the corresponding receptors; IgG A, IgG aggregation; NIR775, an H_2S-inert fluorophore; Cy7Cl, a cationic cyanine dye; HyNPs, hybrid micellar nanoparticles; NPs, nanoparticles; FRET, fluorescence resonance energy transfer; IONPs, iron oxide NPs; P, FITC-labelled GzmB substrate peptides; LICOR, IRDye-800CW; EB-NS, prepared by the layered pigment $CaCuSi_4O_{10}$ (Egyptian Blue, EB) via ball milling and facile tip sonication into NIR fluorescent nanosheets; DSNP@MY-1057-GPC-3, active targeting antibody glypican-3 (GPC-3) was conjugated with DSNP@MY-1057; MY-1057, a common cyanine dye; HCC, hepatocellular carcinoma; DSNP, lanthanide downshifting NPs (DSNPs): β-$NaYF_4$ @$NaYF_4$:1%Nd; Pb-Ag_2S ODs, lead doped Ag_2S quantum dots; SPNs, semiconducting polymer NPs.

response in the presence of the SARS-CoV-2 S protein (S) receptor-binding domain (RBD), compared to the PBS solutions containing SARS-CoV-1 S RBD, (Middle East respiratory syndrome coronavirus) MERS S RBD, influenza viral hemagglutinin subunit (HA1), or serum albumin (HSA) (Fig. 4a). On the other hand, due to the biofouling effects, the NIR fluorescence response of this sensor in biological fluids was significantly attenuated (Fig. 4b). This will make viruses indistinguishable from real samples. However, by surface passivation with hydrophilic polymers (Fig. 4c), this ACE2-SWCNT nanosensor maintained its sensing capability in the biofluids exposed to 35 mg/L SARS-CoV-2 virus-like particles, exhibiting a 73% fluorescence-enhanced response (Fig. 4d) within 5 s. After detection of recombinant proteins and their validation in pseudovirus systems, this sensor is promising to detect real SARS-CoV-2 virus. However, many better-developed approaches are still expected to confirm the test effects.

The SWCNTs are one-dimensional (1-D) materials with a diameter smaller than 2 nm, but the length can be tuned to as long as several mm or even longer. Compared to common NIR fluorophores, the photostability of SWCNTs tends to be exceptionally stable. [77] Although the pollution of SWCNTs-based sensors to the environment is not avoidable [78], optimization of synthesis methods for tuning the surface conditions (such as surface passivation [79]), and other physical properties (such as the longer length [80]) may reduce the environmental damage.

3.2. Promising nanobodies

Antibodies are widely used in biosensors as bioreceptors to target the analytes. However, the size of the traditional antibody is relatively large, and the corresponding steric hindrance is also large. This limits the high-precision detection in some cases and causes the inaccuracy of the test results. Nanobodies are normally smaller than 15 kDa and have sizes of ~2.5 nm in diameter and ~4 nm in height. Compared to traditional antibodies, they have advantages such as high stability, deep tissue penetration, and quick clearance from circulation. The nanobodies can be the recombinant variable domains of heavy-chain-only antibodies, which have the potential to play a role as receptors for the NIR fluorescent nanosensor, though no related work is reported. Guo et al. used nanobody-functionalized organic electrochemical transistors with a modular architecture for the rapid analysis of specific SARS-CoV-2 antigens in complex bodily fluids (Fig. 5). The nanosensors combine a solution-processable conjugated polymer and nanobody-SpyCatcher fusion proteins on disposable gate electrodes by organic electrochemical transistors (OECT) signals. This nanobody is promising to be extended as a bioreceptor detect SARS-CoV-2 antigen if the corresponding specific nanobody is available to conjugate with the NIR fluorescent nanomaterials. Nanobodies normally can target SARS-CoV-2 infections at ultra-low doses, [81] which will show advantages to reducing the biohazard release from the sampling progress.

3.3. Artificial receptors

The specific sensing of SARS-CoV-2 is normally based on the surface chemistry design of substrate and transducers using bioreceptors including deoxyribonucleic acid (DNA)/RNA aptamers [83–87] or enzymes such as ACE2, etc. [88] However, these bioreceptors are not cost-effective. During functionalization, the binding ability of a bioreceptor to the virus may be unstable due to external processing such as immobilization and device interface. Furthermore, the sensing cycle involves complex manufacturing processing steps. This includes protein synthesis/purification and washing steps that require extensive chemical reagents. On the other hand, nanomaterials or polymers are promising artificial bioreceptors based on self-organization and structural adaptation, which can improve stability, reduce cost, and waste release. By appropriately tuning the surface as a flexible array of radially aligned organic molecules, the nanomaterials or polymers can be used as artificial receptors to SARS-CoV-2, where identification can be achieved based on surface interactions. For example, the nanoparticle corona interface can recognize SARS-CoV-2 proteins without any antibodies or other biological receptors. Cho et al. developed a corona phase molecular recognition (CoPhMoRe) system based on the adsorption of Poly (ethylene glycol) (PEG)-phospholipid heteropolymers onto NIR fluorescent SWCNTs to recognize the N and S proteins of SARS-CoV-2, facilitating label-free NIR fluorescence sensing. [89] Different structures between PEGylated lipid heteropolymers and SWCNTs have been investigated in search of optimized sensors (Fig. 6a,b). Among the sensors, 18:0 (1,2-distearoyl-sn-glycero-3-phosphoethanolamine-N-[methoxy(polyethylene glycol)– 1000] PEG1000 PE/SWCNT (nanosensor ii) and 14:0 (1,2-distearoyl-sn-glycero-3-phosphoethanolamine-N-[methoxy(polyethylene glycol)– 2000) PEG2000 PE/SWCNT (nanosensor vi) had the most sensitive responses to N and S proteins, respectively (Fig. 6c). Both nanosensors showed up to 50% signal response within 5 min of viral protein injection, with detection limits of 48 fM and 350 pM for N and S proteins, respectively, by using small amounts of samples. The instrumentation was performed based on a fiber-optic platform, which was effective for the analysis of SARS-CoV-2 in human saliva conditions. The development of nano/polymer receptors for recognizing SARS-CoV-2 is expected to simplify the functionalization of the NIR fluorescent nanosensors and it may also benefit environmental protection.

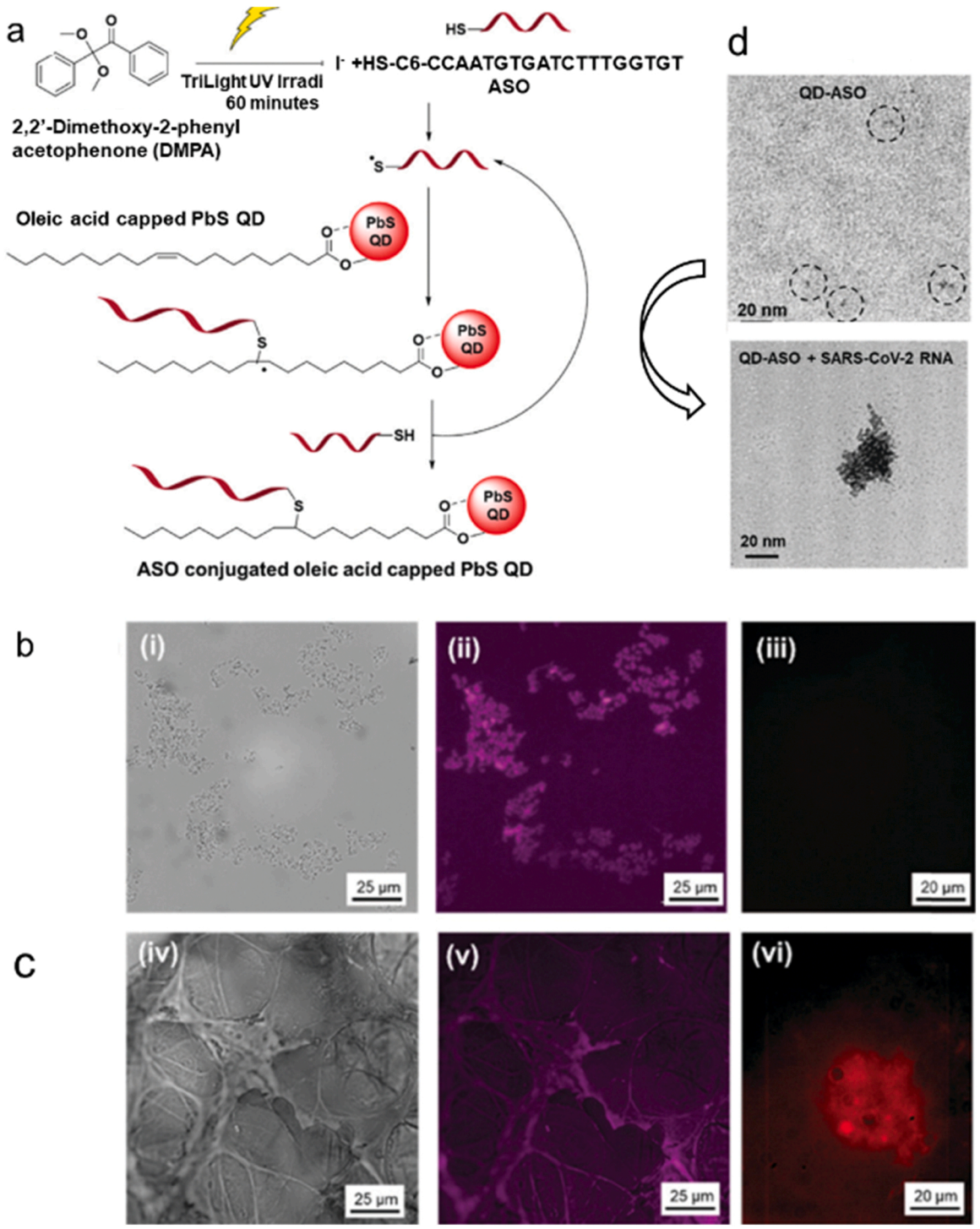

Fig. 3. (a) The conjugation of thiolated ASO with the oleic acid capped Pbs QDs. Imaging of the lung tissues (b) in the absence and (c) presence of SARS-CoV-2 viral RNA while injected with PbS QD-ASO; i and iv are the bright-field images; ii and v show the auto-fluorescence from the biological tissues; iii and vi present NIR-II imaging of the tissues; (d) TEM image of the sensor in the absence (up) and the presence of SARS-CoV-2 (down).
Reprinted from ref.[72] with permission from Royal Society of Chemistry (copyright 2021).

4. Antibody test

Antibodies including IgM, IgG, and IgA against the S protein and the subunits can be tested within 1–3 weeks after SARS-CoV-2 infection.[90, 91] People who were infected by SARS-CoV-2 could have a positive antibody test result. NIR fluorescent nanosensors have been developed based on the amplification of the NIR fluorescence of organic dyes. For instance, the plasmonic gold (pGOLD) substrate is composed of nanoscale gold islands with abundant nanogaps,[92] which can significantly enhance the fluorescence of dyes due to the plasmonic resonance and local electric field enhancements. Liu et al. developed an IRDye800 (emission at ca. 800 nm, which is a common NIR fluorescent dye used for labeling oligonucleotides) labeled anti-human IgG and CF647 (a cyanine-based far-red fluorescent dye) (emission peak at ca. 660 nm) labeled anti-human IgM for detection of IgG and IgM against S1 (Spike Glycoprotein (S1) is a recombinant antigen which contains amino acids

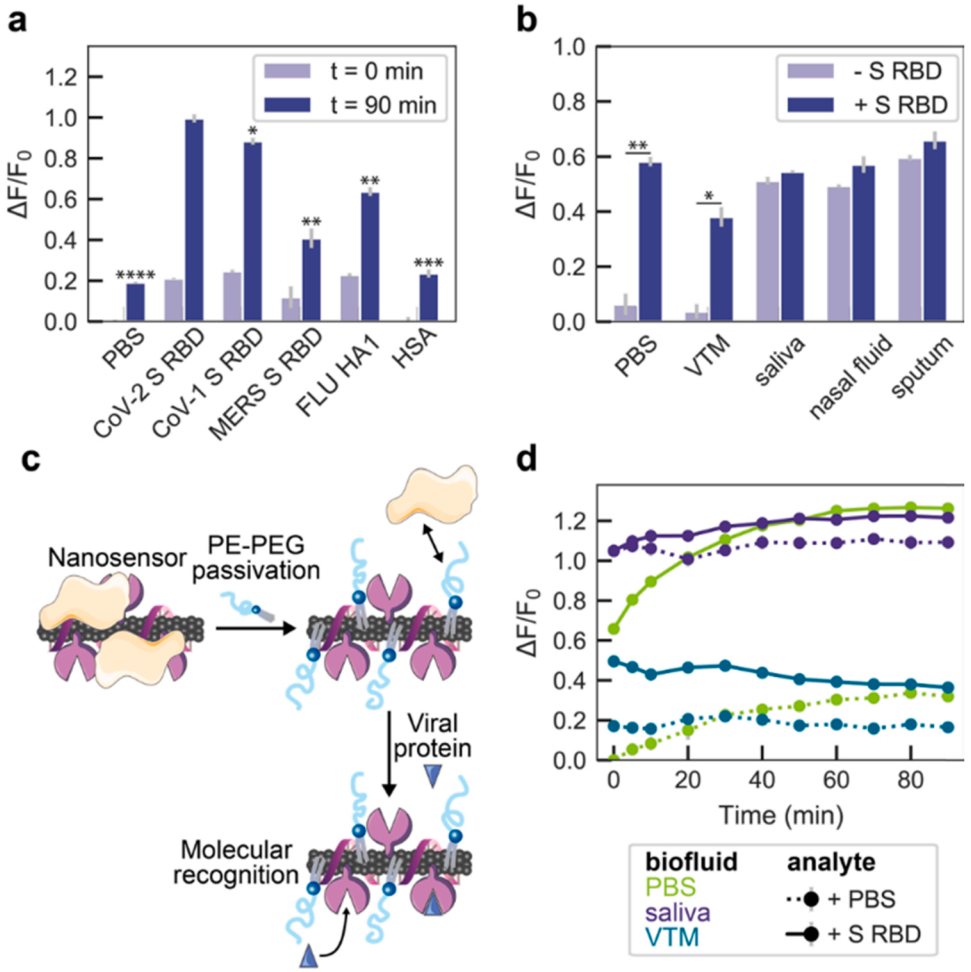

Fig. 4. The selectivity and sensitivity of ACE2-SWCNT NIR fluorescent nanosensor. (a) Normalized fluorescence ($\Delta F/F_0$) change of the 1130 nm SWCNT emission peak for the ACE2-SWCNT nanosensor at 0 and 90 min after exposure to 10 mg/L of viral protein panel shows the sensor has a selectivity of SARS-CoV-2 S RBD against other samples in Phosphate-buffered saline (PBS) solutions: SARS-CoV-2 spike RBD (S RBD), SARS-CoV-1 S RBD, MERS S RBD, and FLU (FLU refers to an infectious disease caused by influenza viruses) HA1. (b) The sensor response at 90 min after exposure to 1 μM S RBD in the presence of 1% relevant biofluids is not selective: viral transport medium (VTM), saliva, nasal fluid, and sputum. (c) The biofouling of the NIR nanosensor with proteins present in relevant biofluids, mitigated by passivation using a PE-PEG polymer (phosphatidylethanolamine phospholipid with a 5000 Da PEG chain).
(d) Response of PE-PEG passivated NIR nanosensor to 500 nM S RBD in the presence of PBS, 10% VTM, or 1% saliva; Reproduced with permission from ref.[76] copyright (2021) American Chemical Society.

1–674 of subunit 1) and RBD antigens on pGOLD in human serum and saliva at NIR and visible range simultaneously. [93] The enhanced signals and two-color readout facilitate discrimination of the different antibodies, which is accurate to almost all investigated COVID-19 patients (collected more than 14 days after infection) and has a specificity of 99.78% in detecting IgG and IgM subtypes against S1 antigen. The increased signal-to-background ratio on pGOLD offers highly specific antibody tests to avoid false-positive results. The combination of such nano surfaces with NIR fluorescent dyes provides signal magnification for sensitive detection of SARS-CoV-2. Notwithstanding, compared to NIR fluorescent nanomaterials, organic dyes tend to be more toxic. To improve this problem, Chen et al. developed a NIR emissive aggregation-induced emission (AIE) dye (BPBT) loaded polystyrene (PS) nanoparticle (AIE810NP: Excitation 680 nm; Emission: 810 nm) (Fig. 7a), which were functionalized with SARS-CoV-2 antigen (AIE810NP-SARS-CoV-2 antigen) (Fig. 7b). A portable reader was connected to read the signal response (Fig. 7c) by fabricating the sensor as a NIR-lateral-flow strip (Fig. 7d). The method achieves a diagnostic accuracy of 78% and 95% for IgM and IgG, respectively. Compared to the less accurately commercial gold nanoparticle (AuNP)-based test strip (41% and 85% of accuracy after 8–15 days), this NIR fluorescent nanodevice more accurately detected IgM and IgG against SARS-CoV-2 within 1–7 days after symptoms appear. It also facilitates more effective detection of IgM and IgG against SARS-CoV-2 in clinical samples compared to the traditional optical strips. The development of organic molecules as AIE materials not only reduces the toxic release due to the larger size and higher stability but also may significantly enhance the NIR fluorescence facilitating more sensitive detections. [94–96] The more sensitive the method, the smaller the sample volume required, or the simpler the sample handling process. Once the sensor is sensitive enough, the RNA/protein extraction may even be avoided. [97] Therefore, more sensitive detection strategies based on NIR fluorescent nanosensors for the detection of SARS-CoV-2 are expected to benefit environmental protection.

5. Emerging biomarkers

Many diagnostic methods are static and cannot differentiate between live and non-live viruses. To confirm SARS-CoV-2 infections, multiple patient samples are often collected at different times. The methods for real-time diagnosis of SARS-CoV-2 are very important to decrease the frequency of the test. Dynamic analysis of some biomarkers is a powerful tool for real-time disease diagnosis. [99].

The 5' two-thirds of the viral genome of SARS-CoV-2 encodes two overlapping polyproteins, pp1a and pp1ab, which generate replicate polyproteins that are processed by two viral proteases, the papain-like protease (PLpro) and main protease (Mpro). [100] The two proteases are the basis for the replication of SARS-CoV, which can be used as important biomarkers for the detection of SARS-CoV-2. Pu et al. designed an activatable NIR fluorescence (NIRF) molecular probe (SARS-CyCD) for the real-time detection of the protease in living mice (Fig. 8). This sensor not only can sensitively detect Mpro in the lungs of living mice after intratracheal administration but also can detect SARS-CoV-2 infection through optical urinalysis. This study constructed a low-toxic in vivo NIR fluorescent sensor for biomarker analysis, which has the potential to reflect real-time SARS-CoV-2 infection.

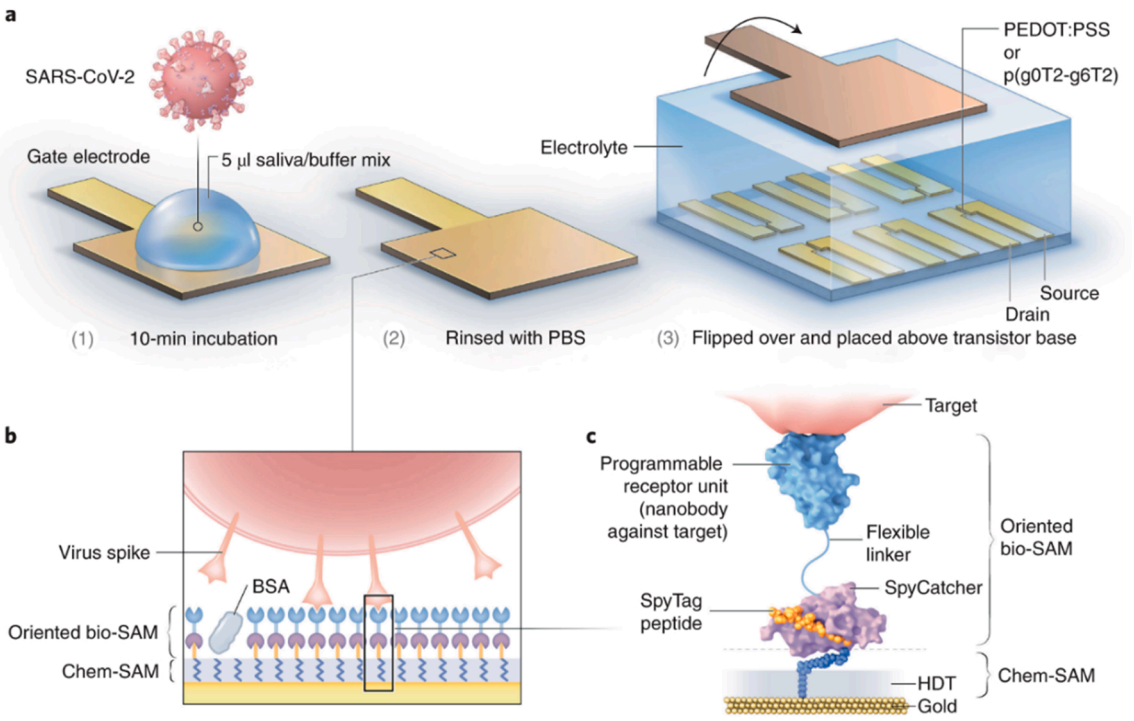

Fig. 5. a, Operation progress. The gate electrode is exposed to the mixture of the sample and binding buffer (1), washed by PBS (2), OECT signal acquisition (3). b, The construction of gate functionalization layers. The biological self-assembled monolayer (SAM) (Bio-SAMs) and a combined chemical SAM (Chem-SAMs) on the gate electrode surface. c, Molecular architecture of the nanobody recognization system: The chem-SAM is formed by SpyTag peptide that is coupled to the HDT monolayer; The nanobody–SpyCatcher fusion protein attaches to this layer through the autocatalytic formation of a covalent SpyCatcher–SpyTag bond.
Reprinted from ref.[82] with permission from Springer Nature (copyright 2021).

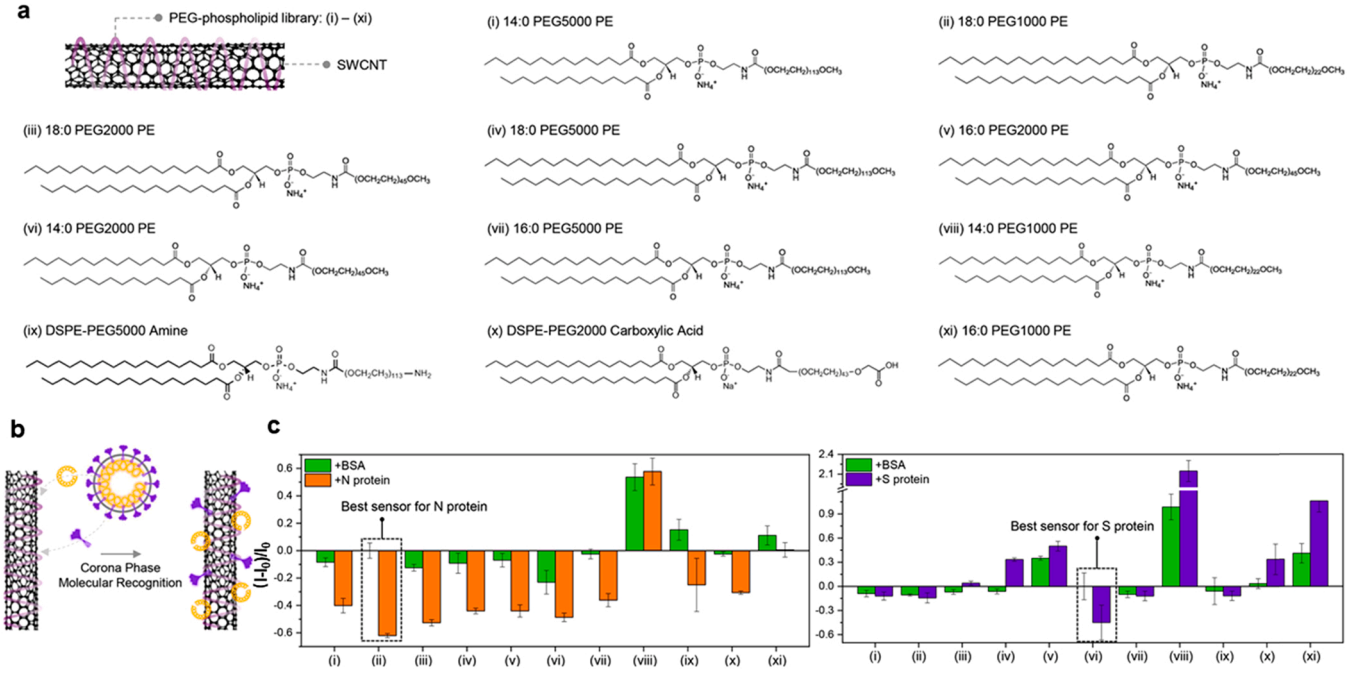

Fig. 6. (a) PEG-phospholipid library for CoPhMoRe-based SWCNT nanosensors. (b) Scheme for CoPhMoRe system to detect SARS-CoV-2 proteins using PEG-phospholipid/SWCNT nanosensors on N and S viral proteins. (c) Screening results of the integrated normalized response of nanosensors library on N protein (top) and S protein (bottom). Dashed lines indicate the best nanosensor for each protein. nanosensor ii and nanosensor vi showed the most remarkable fluorescence decreases in 50–70%, indicating these two sensors have optimized polymer receptors.
Reprinted from ref.[89] with permission from copyright (2021) American Chemical Society.

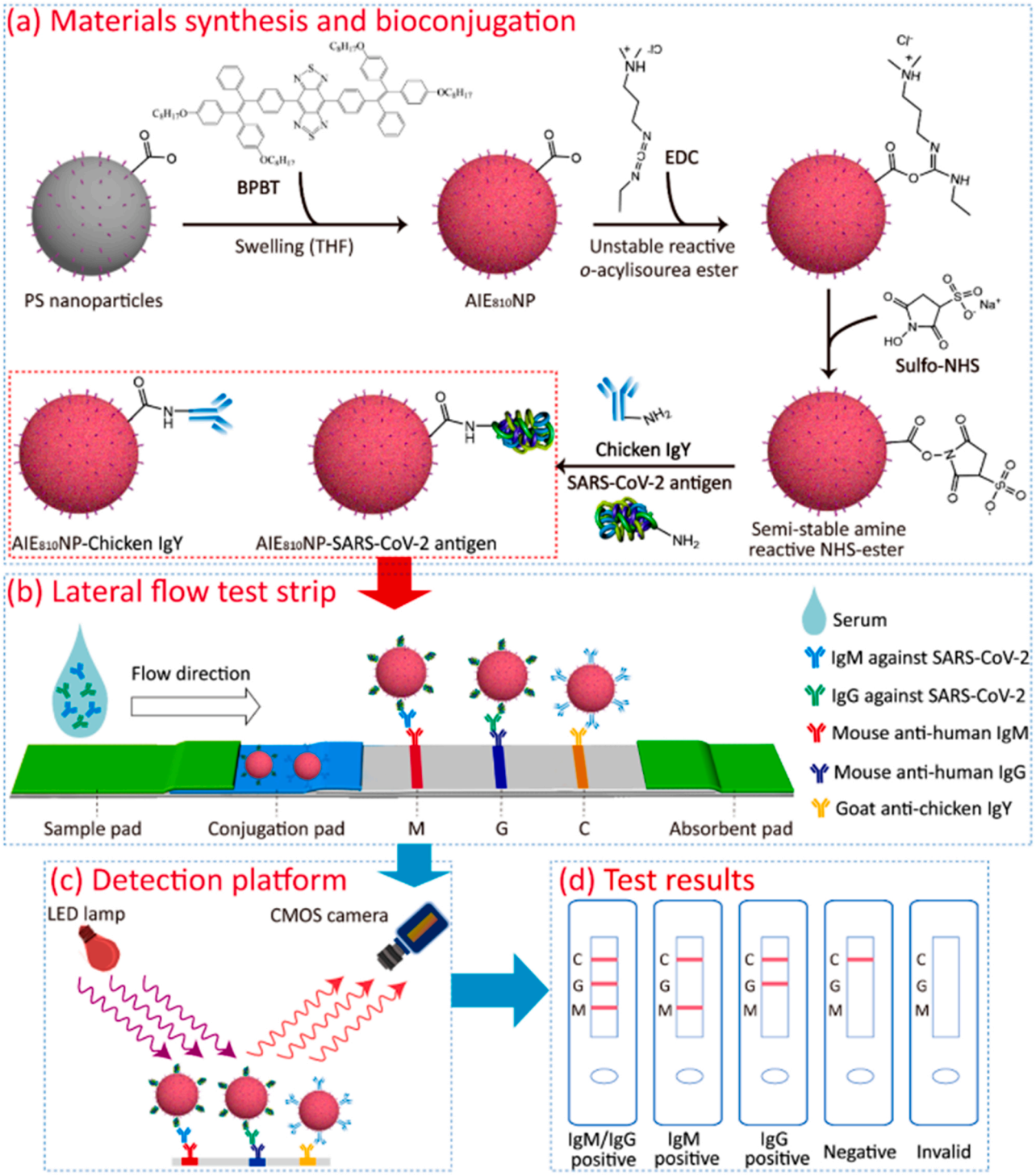

Fig. 7. (a) Synthesis and conjugation of AIE810NP with SARS-CoV-2 antigen and chicken immunoglobulin Y (IgY). (b) A lateral-flow test strip was fabricated for the detection of IgM and IgG. (c) The portable reader contains a 680 nm LED lamp (excitation), a complementary metal-oxide-semiconductor (CMOS) camera, and a set of optics. (d) Scheme for different test results: coexistence of M line, G line, and C line indicate IgM/IgG positive; both M line and C line appear, which mean IgM positive; coexistence of G line and C line represent IgG positive; The presence of C line only shows IgM/IgG negative; No line reveals an invalid test strip. Reproduced with permission from ref.[98] copyright (2021) American Chemical Society.

SARS-CoV-2 infection elicits inflammatory responses and triggers various inflammatory biomarkers. Therefore, various inflammatory biomarkers such as C-reactive protein, interleukin-6, procalcitonin, and ferritin have been reported to be associated with this infection. [102] Combined with the analysis of these biomarkers related to the viral components by NIR fluorescent nanosensors, the low levels of SARS-CoV-2 infections may be analyzed based on the inflammatory response, which has been missed by many traditional testing. [103] Although no NIR fluorescent nanosensors simultaneously analyze biomarkers attributed to the inflammatory response and viral components, the combination of these analyses in the diagnosis of COVID-19 will hopefully realize real-time infection diagnosis avoid frequent testing of the same case. [104].

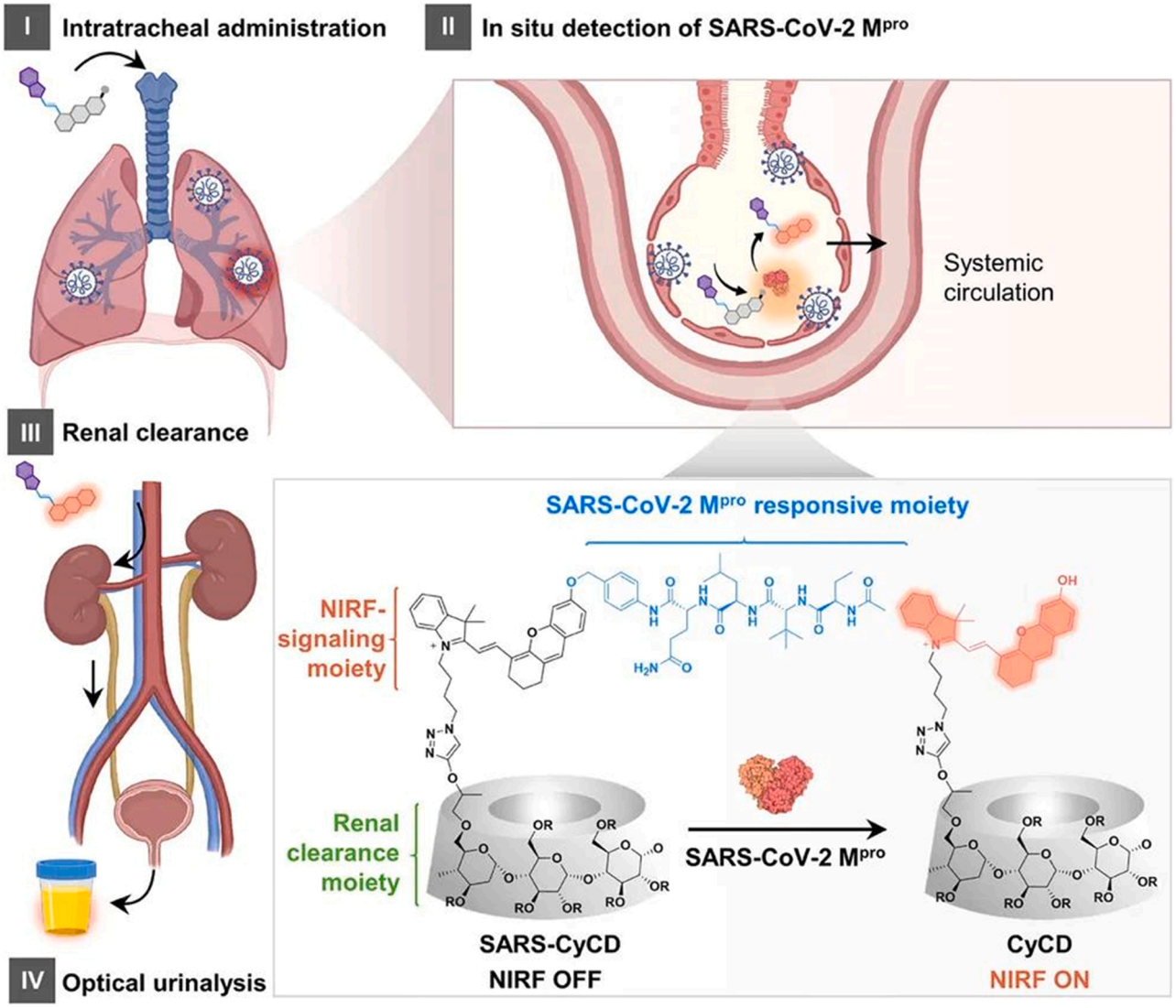

Fig. 8. In vivo detection of SARS-CoV-2 Mpro by renal-clearable NIR fluorescent sensors. The peptide substrate of SARS-CyCD was specifically cleaved by Mpro, activating NIRF signal and liberating the renal-clearable fluorescent fragment (SARS-CyCD).
Reproduced with permission from ref. [101] copyright (2021) American Chemical Society.

6. Potential improvement for the NIR fluorescent nanosensors

6.1. Promising diagnosis devices

Combined with point of care (POC) devices, the detection of SARS-CoV-2 by NIR fluorescent nanosensors tends to be more accessible to the public. Although such devices have not been designed for NIR fluorescent nanosensors, VIS fluorescent nanosensors combined with POC devices have already been investigated, which gives insight for further research. Guo proposed a 5 G (5 G is the fifth generation technology standard for broadband cellular networks)-enabled VIS fluorescent sensor for quantitative detection of S and N protein of SARS-CoV-2 by using mesoporous silica ($mSiO_2$) encapsulated up-conversion NPs (UCNPs) as fluorescent labels (Fig. 9a, c), i.e., UCNPs@$mSiO_2$. [105] UCNPs@$mSiO_2$ show emissions around 542 nm and 657 nm under 980 nm NIR laser irradiation (1.3 W/cm^2). The sensor detected S protein with a detection limit of 1.6 ng/mL and N protein (NP) with a detection limit of 2.2 ng/mL using a lateral flow device connected with a 5 G phone. The test results were expected to be transmitted to the fog layer of the network and the 5 G cloud server for big data analysis (Fig. 9b). Then, the monitoring results could be noticed by their families and shared by others. Such a system may be extended for the NIR fluorescent sensors by replacing VIS fluorescent labels with the NIR fluorescent nanomaterials by appropriate excitations. [106] For example, optimizing the NIR fluorescent nanomaterials in Table 2 may provide excellent candidates for this alternative. However, some of these nanomaterials are not biocompatible after synthesis and require further functionalization. On the other hand, some materials are directly obtained by the green synthesis method, but the low quantum yield (QY) may make it difficult to develop a sensitive sensor. Therefore, the synthesis, application, and environmental impact of these materials should be comprehensively considered.

6.2. Hybrobic NIR fluorescent nanomaterials from organic-phase synthesis

Many NIR fluorescent nanomaterials are synthesized from organic solvents. The release of large amounts of organic solvents is inevitable. Furthermore, most of these nanomaterials obtained from organic phase synthesis are hydrophobic. For example, most SWCNTs, rare-earth-based NPs, inorganic nanoshells, and various semiconductor QDs/NPs cannot directly dissolve in biocompatible media after synthesis.

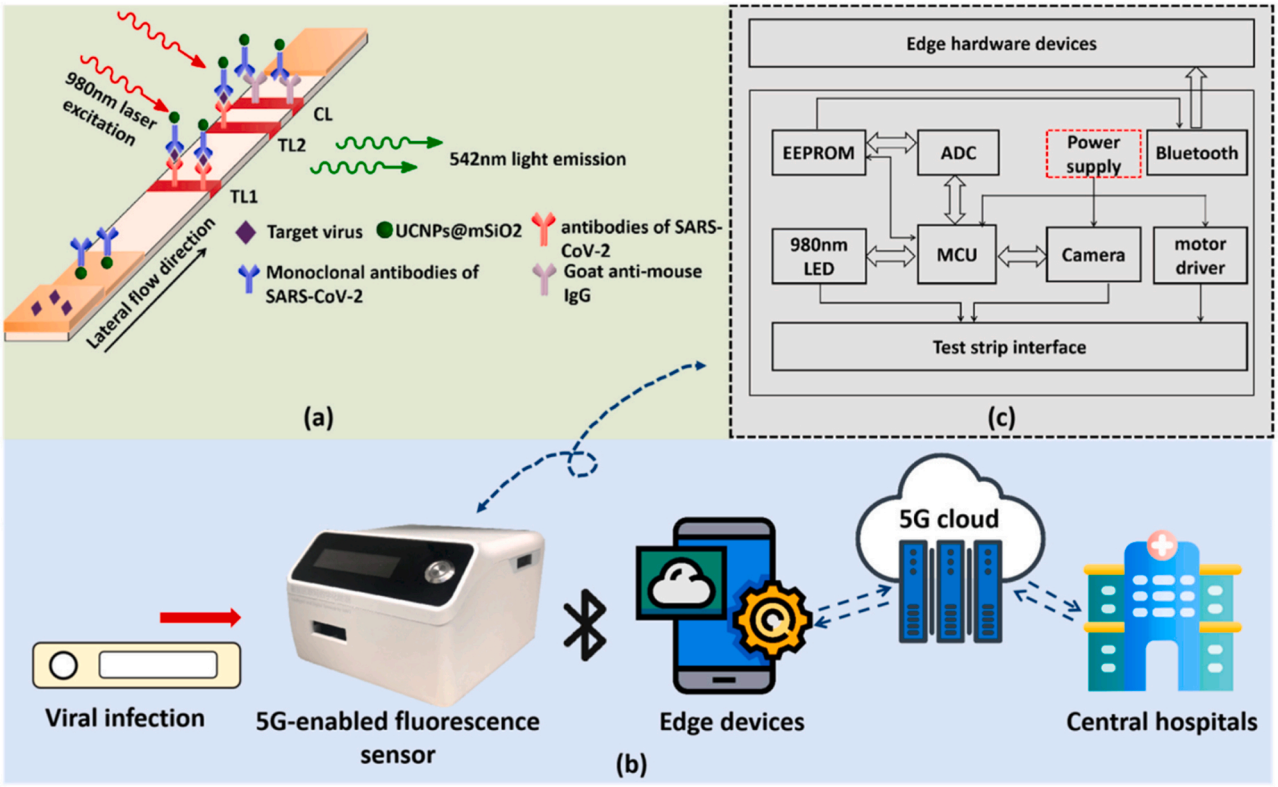

Fig. 9. (a) The UCNPs based lateral flow assay in detection of SARS-CoV-2. (b) A proposed 5 G-enabled VIS fluorescence sensor. (c) The circuit and hardware of the proposed sensor. The 5 G-enabled VIS fluorescence sensor includes a focusing lens, a high-speed camera, a 980 nm wavelength optical filter, a motor driver, a 980 nm light-emitting diode (LED) module, a Bluetooth model, and a microcontroller unit (MCU) pre-embedded with control and processing modules. The images captured by the camera could be grayed out and de-contextualized by the data processing module. The obtained T/C value is used to determine the concentration of the virus. Reproduced with permission from ref.[105] copyright (2021) ELSEVIER.

Table 2
Promising nanomaterials for designing NIR fluorescent sensors of SARS-CoV-2.

NPs	Excitation	Emission	QY	Production	Possible pollutants	Previous applications	Ref.
SWCNTS	808 nm	1500–1700 nm	0.01%	Laser vaporization synthesis; DSPEmPEG(5k) functionalization	Susfactants	In vivo imaging	[107]
SWCNTS	561 nm	990 nm, 1130 nm	0.6–1.3%	CoMoCAT® process	Susfactants	Biosensing	[108]
Rare earth based DCNPs	980 nm	> 1500 nm	0.27%–0.73	Solvent Thermal/Hydrothermal; Functionalization	Organic solvent	Biological imaging	[109–112]
Rare earth based DCNPs	808 nm	1000–1700 nm	Not mentioned	Solvent Thermal/Hydrothermal; Functionalization	Organic solvent	Tumor biomarker imaging	[113,114]
Rare earth UCNPs	980 nm	800 nm	~ 7.9%	Sovent Thermal/Hydrothermal; Functionalization	Organic solvent	Lateral flow detection of avian influenza virus	[115–117]
Inorganic Nanoshells	808 nm	1064 nm	Not mentioned	Sonochemical Synthesis; Functionalizaiton	Functionalized agents	Cancer therapy	[118]
Polymers	1064 nm	940 nm	Not mentioned	Emulsions method; Functionalizaiton	Organic solvent	PTT; Photoacoustic imaging	[119]
Semiconductor QDs	808 nm	1039–1600 nm	2.2–22%	Organic phase synthesis; Functionalization	Organic solvent	Fluorescence imaging	[71,120]
CDs	808 nm	900–1200 nm	0.4%	Hydrothermal synthesis	None	PTT	[121]
AuNCs	808 nm	1050 nm	0.11%–0.27%	Green aquesous synthesis	None	Tumour or bone targeted imaging	[122,123]
AIE NPs	793 nm	1030–1600 nm	11.5%	Nanoprecipitation method	Organic solvent	Blood vessel imaging	[124]

Note: Down-conversion NPs, DCNPs; PEG-CSQDs, core/shell lead sulfide/cadmium sulfide (CdS) quantum dots (CSQDs) branched by Polyethylene glycol (PEG); AuNCs, gold nanoclusters; AIE NPs, NPs with aggregation-induced emission; PTT, photothermal therapy; CDs, carbon dots; AuNCs, gold nanoclusters.

Necessary strategies are needed to increase their water dispersibility. [125] Some of these hydrophobic nanomaterials can be covalently attached to hydrophilic groups by phase transfer methods or other protocols, but the processes may destroy the surface activity of nanomaterials, resulting in partial loss of properties such as fluorescence. On the other hand, non-covalent methods may preserve the inherent properties of these NIR fluorescent materials. For example, surfactants such as sodium dodecyl sulfate (SDS) have been introduced to link with hydrophobic SWCNTs in aqueous solutions through π-electron, van der Waals, or electrostatic interactions, etc., resulting in bunching of biocompatible nanomicelles in aqueous solutions. [126] The binding between surfactants and SWCNTs does not depend on the breaking and

reorganization of hydrogen bonds. The fluorescence properties may be preserved. Notwithstanding, the increased surfactants increase the waste release. Their safety during and after use for the detection of SARS-CoV-2 in vitro/vivo remains an issue.

6.3. Hydrophilic NIR fluorescent nanomaterials from water-phase synthesis

The non-toxic, biocompatible, water-soluble, and highly fluorescent NIR fluorescent nanomaterials tend to reduce waste release. Many NIR fluorescent semiconductor ODs/NPs are synthesized from toxic heavy metal precursors, organic solvents, and/or high temperatures. These conditions are not environmentally friendly enough. However, some metal-semiconductor-based nanomaterials can be produced by green methods and exhibit excellent biocompatibility. For example, Ag-Ag_2S-based NPs can be prepared by a simple green synthetic route. [53] The coordinating molecules are produced from aqueous extracts of roasted coffee and the Ag-Ag_2S are obtained from aqueous solutions at room temperatures. Notwithstanding, the optimized reaction conditions only produce weak fluorescent Ag-Ag_2S NPs (Emission:1250 nm; Excitation: 784 nm) with a QY of 0.1%. The fluorescence may not be bright enough for satisfying the sensitive detection of SARS-CoV-2.

Metal nanoclusters (NCs) are ultra-small nanomaterials (<3 nm) containing a small number of metal elements and stabilized by protective ligands. Most of them can be obtained by the green synthesis method. Among the NCs, NIR fluorescent gold NCs (AuNCs) can be obtained by a one-pot method in an aqueous solution at room temperature or relatively low temperature (< 60 °C) simply by mixing metal pressures, stable ligands, and reducing agents. For example, NIR fluorescent glutathione-stabilized AuNCs (GSH-AuNCs) could be fabricated by only glutathione (GSH), chloroauric acid ($HauCl_4$), and sodium borohydride ($NaBH_4$) throughout the synthesis. No additional surface functionalization is required, but the product is already biocompatible. In the application process, there are negligible toxic effects. Li et al. have developed NIR fluorescent GSH-AuNCs that show emission at 1050 nm with 808 nm excitation and the QY is 0.27%.[122] The fluorescence brightness may satisfy the detection of SARS-CoV-2 in vivo and in vitro. However, to satisfy the sensitivity and accuracy of the diagnosis, it is necessary to further improve the QY of NIR fluorescent NCs. We have investigated a variety of effective methods to significantly improve the QY of NCs emitting in the range from VIS to NIR(I) through element doping, immobilization of surface ligands, AIE method, etc. [127] Although these strategies have not yet been applied to NIR fluorescent AuNCs with relatively long emission wavelengths (>1000 nm), the combination of these enhancement strategies with the synthesis of NIR fluorescent NCs may significantly improve their QY.

Carbon nanodots (CDs) are small carbon NPs (<10 nm) with some form of surface passivation. Many CDs can be produced directly in aqueous solvents from green sources such as fruit juices or carbon-containing natural products. These CDs can be directly biocompatible after synthesis. On top of that, the materials tend to be degradable after use, making them less harmful to the environment than nanomaterials that contain toxic elements. [121] Li et al. fabricated a NIR-II-emitting CDs-based nanosensor triggered by an 808 nm laser by a hydrothermal method from watermelon juice at 190 °C for 3 h. [128] The CDs show emissions within the range of 900–1200 nm that possess QY as high as 0.4%). These NIR fluorescent CDs have proven to be effective probes for in vivo renal-excreted imaging. It may also satisfy the NIR fluorescent imaging of SARS-CoV-2.

The water-soluble NIR fluorescent nanomaterials obtained by water-phase synthesis, are relatively safe, cheap, and energy-saving. These nanomaterials are worthy of continued research and investigation for the green detection of SARS-CoV-2.

6.4. Hydrophilic NIR fluorescent AIE NPs

Some AIE luminogens (AIEgens) emit intensely brighter fluorescence after aggregation due to the restriction of the intramolecular motion (RIM) mechanism, but most of these AIEgens were obtained from organic molecules and cannot be dissolved in the aqueous solvent until further modifications. [129] Li et al. constructed the organic-solvent-soluble AIEgens into hydrophilic NPs (AIE NPs) by a nanoprecipitation method using amphiphilic copolymers (DSPE--PEG_{2000}) as the doping matrix. [124] The biocompatible matrix enabled the AIE NPs to exhibit excellent dispersibility in aqueous media and a satisfactory blood circulation time due to the surface PEG. The AIE NPs show excellent performance for NIR-IIb fluorescence (Excitation, 793 nm) imaging of brain vasculature in living mice. The biocompatible AIE NPs may be extended for the detection of SARS-CoV-2 and improve the sensing sensitivity. However, further investigation of greener resources may still be required. In addition, many AIE materials based on organic molecules exhibit relatively shorter NIR fluorescence (<800 nm) and higher toxicity. The longer the wavelength, the fewer the background value of the interferences exhibited. [130].

With proper design, NIR fluorescent nanomaterials can have longer emission wavelengths and lower toxicity. Obtaining AIE fluorescent nanomaterials from dispersed NIR fluorescent nanomaterials as alternatives for organic molecules, or utilizing the energy transfer of two photons to obtain combinatorial systems with brighter fluorescence, may be promising for the construction of NIR fluorescent nanosensors for SARS-CoV-2 infection diagnosis.

6.5. Sensor regeneration

Reusability is important for developing sustainable sensors since it can reduce waste release. However, most sensors are not reusable after mixing with the target solution. Therefore, it is highly desirable to develop a recyclable or regenerated NIR fluorescent nanosensor for SARS-CoV-2 detection. Although the reusability of NIR fluorescent nanosensors for the detection of SARS-CoV-2 had not been reported, some other NIR fluorescent sensors were found to be reproducible. For example, electrospun nanofibrous membranes (ENMs) with large surface areas are ideal solid substrates for restoring and regenerating a NIR fluorescent nanosensor. Wang et al. fabricated a reusable NIR fluorescence sensor for the detection of heme proteins based on conjugated polymer-doped electrospun nanofibrous membranes. [131] Since heme proteins were adsorbed on the nanofibers based on a non-covalent hydrophobic interaction, the sensor could be recovered by simply immersing in 50 mL PBS solutions for 20 min. More than 90% signal intensity of the nanosensor remained after 9 regeneration cycles, indicating excellent reusability of this sensor. Zhang et al. developed a reusable NIR fluorescent nanosensor based on recyclable upconversion-fluorescence indicator papers consisting of upconversion nanorods and plasmonic nanostructures, which were fabricated by electrospinning. [132] Human-body fluids containing different concentrations of riboflavin are used as target solutions. After the detection, the sensor can be regenerated by removing the target solution attributed to its superhydrophobicity and flexibility, and this indicator paper is stable after 100 cyclic tests. Among NIR fluorescent nanomaterials, SWCNTs are known for their excellent thermal stability. [42] The detachment of absorbed analytes from the SWCNTs can be realized by heating, but the property of the SWCNTs-based sensor may not be destroyed. This strategy has been successfully employed for the regeneration of the NIR fluorescent nanosensor after the detection of acetic acid in the gaseous phase. [133] This inspired us that attaching NIR chromophores on regenerated surfaces or employing thermally stable NIR fluorescent nanosensors may hold promise to fabricate a regenerative sensor for the detection of SARS-CoV-2. Furthermore, If the viral RNA, antigens, viral particles, or antibodies are broken down in certain conditions without the sensor being affected, these conditions could be a

way to study renewable sensors in the future.

7. Conclusions and prospects

The reported NIR fluorescent nanosensors and the corresponding POC devices are promising to detect SARS-CoV-2 infections accurately. These sensors were fabricated by chromophores originating from NIR fluorescent nanomaterials or dyes loaded by nanomaterials. The bioreceptors (or artificial receptors) are attached to these sensors for the recognition of the virus. With the assistance of signal amplification using specific nanostructures such as plasmonic gold, more sensitive and convenient detections can be achieved. NIR fluorescent nanosensors are expected to become home-sharing detection methods through internet technology by the combination with POC devices.

Some of the methods have been validated by RNA, recombinant protein, or/and pseudovirus detection. For real SARS-CoV-2 sample analysis, continuing efforts are still needed for the modification of the NIR fluorescent nanosensor more environmental-friendly. The improvements for NIR fluorescent nanosensors can be made from the following aspects: (1) More fluorescence enhancement strategies can be introduced to various green synthesis protocols for obtaining biocompatible and highly fluorescent NIR fluorescent nanomaterials. The effective strategy will improve the sensitivity of the corresponding sensor and reduce the waste release. (2) More regenerated strategies can be studied for recovering the sensor after the detection of the virus. Then, the disposable materials may be decreased. (3) Real-time and complex analysis of SARS-CoV-2 biomarkers by NIR fluorescent nanosensors are not only promising to directly reflect the activity of the virus, but also reduce the test frequencies. (4) The mutation of the virus significantly interfered with accurate testing, which may invalidate the recognition element. More flexible recognization elements, such as the artificial receptors, which are tunable according to the new virus RNA, antigen, or antibody should be investigated. Nanomaterials/polymers can be designed to include chromophores and artificial receptors, which may possess NIR fluorescence and tunable recognition capabilities for SARS-CoV-2. For example, a new method may be designed to identify mutant viruses by simply changing the sensor surface without altering sensing strategies.

At present, the existing detection technologies are very necessary. But from a long-term perspective, the development of sustainable detection methods is our ultimate goal. By further improving the test sensitivity, reducing material toxicity, increasing the reusability, and decreasing the test frequency, it is reasonable to believe that the optimized NIR fluorescent nanosensor for detecting SARS-CoV-2 can be more sustainable.

Funding

This work is supported by the Liaoning Provincial Department of Education 2021 scientific research funding project (No. LJKZ0818).

Authors' contributions

DL searched the references and wrote the manuscript. ZZ and JS assisted in drafting the manuscript. XM supervised the manuscript. All authors read and approved the final manuscript.

Declaration of Competing Interest

The authors declare that they have no known competing financial interests or personal relationships that could have appeared to influence the work reported in this paper.

Availability of data and materials

Any data related to this review are available from the corresponding author on reasonable request.

Acknowledgments

We acknowledge contributions from the members of The First affiliated Hospital of Jinzhou Medical University.

References

[1] K.G. Andersen, A. Rambaut, W.I. Lipkin, E.C. Holmes, R.F. Garry, The proximal origin of SARS-CoV-2, Nat. Med. 26 (2020) 450–452.
[2] A.F. Rendeiro, H. Ravichandran, Y. Bram, V. Chandar, J. Kim, C. Meydan, J. Park, J. Foox, T. Hether, S. Warren, Y. Kim, J. Reeves, S. Salvatore, C.E. Mason, E. C. Swanson, A.C. Borczuk, O. Elemento, R.E. Schwartz, The spatial landscape of lung pathology during COVID-19 progression, Nature 593 (2021) 564–569.
[3] M. Nishiga, D.W. Wang, Y. Han, D.B. Lewis, J.C. Wu, COVID-19 and cardiovascular disease: from basic mechanisms to clinical perspectives, Nat. Rev. Cardiol. 17 (2020) 543–558.
[4] M. Legrand, S. Bell, L. Forni, M. Joannidis, J.L. Koyner, K. Liu, V. Cantaluppi, Pathophysiology of COVID-19-associated acute kidney injury, Nat. Rev. Nephrol. 17 (2021) 751–764.
[5] A.C. Yang, F. Kern, P.M. Losada, M.R. Agam, C.A. Maat, G.P. Schmartz, T. Fehlmann, J.A. Stein, N. Schaum, D.P. Lee, K. Calcuttawala, R.T. Vest, D. Berdnik, N. Lu, O. Hahn, D. Gate, M.W. McNerney, D. Channappa, I. Cobos, N. Ludwig, W.J. Schulz-Schaeffer, A. Keller, T. Wyss-Coray, Dysregulation of brain and choroid plexus cell types in severe COVID-19, Nature 595 (2021) 565–571.
[6] A. Gupta, M.V. Madhavan, K. Sehgal, N. Nair, S. Mahajan, T.S. Sehrawat, B. Bikdeli, N. Ahluwalia, J.C. Ausiello, E.Y. Wan, D.E. Freedberg, A.J. Kirtane, S. A. Parikh, M.S. Maurer, A.S. Nordvig, D. Accili, J.M. Bathon, S. Mohan, K. A. Bauer, M.B. Leon, H.M. Krumholz, N. Uriel, M.R. Mehra, M.S.V. Elkind, G. W. Stone, A. Schwartz, D.D. Ho, J.P. Bilezikian, D.W. Landry, Extrapulmonary manifestations of COVID-19, Nat. Med. 26 (2020) 1017–1032.
[7] J. Cheong, H. Yu, C.Y. Lee, J.U. Lee, H.J. Choi, J.H. Lee, H. Lee, J. Cheon, Fast detection of SARS-CoV-2 RNA via the integration of plasmonic thermocycling and fluorescence detection in a portable device, Nat. Biomed. Eng. 4 (2020) 1159–1167.
[8] C. Wang, Z. Wang, G. Wang, J.Y. Lau, K. Zhang, W. Li, COVID-19 in early 2021: current status and looking forward, Signal Transduct. Target Ther. 6 (2021) 114.
[9] B. Hu, H. Guo, P. Zhou, Z.L. Shi, Characteristics of SARS-CoV-2 and COVID-19, Nat. Rev. Microbiol. 19 (2021) 141–154.
[10] A.R. Chandrasekaran, L. Zhou, K. Halvorsen, Rapid one-step detection of SARS-CoV-2 RNA, Nat. Biomed. Eng. 4 (2020) 1123–1124.
[11] L. Guo, X. Sun, X. Wang, C. Liang, H. Jiang, Q. Gao, M. Dai, B. Qu, S. Fang, Y. Mao, Y. Chen, G. Feng, Q. Gu, R.R. Wang, Q. Zhou, W. Li, SARS-CoV-2 detection with CRISPR diagnostics, Cell Discov. 6 (2020) 34.
[12] D. Shan, J.M. Johnson, S.C. Fernandes, H. Suib, S. Hwang, D. Wuelfing, M. Mendes, M. Holdridge, E.M. Burke, K. Beauregard, Y. Zhang, M. Cleary, S. Xu, X. Yao, P.P. Patel, T. Plavina, D.H. Wilson, L. Chang, K.M. Kaiser, J. Nattermann, S.V. Schmidt, E. Latz, K. Hrusovsky, D. Mattoon, A.J. Ball, N-protein presents early in blood, dried blood and saliva during asymptomatic and symptomatic SARS-CoV-2 infection, Nat. Commun. 12 (2021) 1931.
[13] K.V.-Z. Martin Pavelka, ProfileSam Abbott, Katharine Sherratt, Marek Majdan, CMMID COVID-19 working group, Inštitút Zdravotných Analýz†, Pavol Jarčuška, Marek Krajčí, Stefan Flasche, Sebastian Funk, The impact of population-wide rapid antigen testing on SARS-CoV-2 prevalence in Slovakia, Science 372 (2021) 635–641.
[14] T. Peto, U.C.-L.F.O. Team, COVID-19: rapid antigen detection for SARS-CoV-2 by lateral flow assay: a national systematic evaluation of sensitivity and specificity for mass-testing, EClinicalMedicine 36 (2021), 100924.
[15] R.R. de Assis, A. Jain, R. Nakajima, A. Jasinskas, J. Felgner, J.M. Obiero, P. J. Norris, M. Stone, G. Simmons, A. Bagri, J. Irsch, M. Schreiber, A. Buser, A. Holbro, M. Battegay, P. Hosimer, C. Noesen, O. Adenaiye, S. Tai, F. Hong, D. K. Milton, D.H. Davies, P. Contestable, L.M. Corash, M.P. Busch, P.L. Felgner, S. Khan, Analysis of SARS-CoV-2 antibodies in COVID-19 convalescent blood using a coronavirus antigen microarray, Nat. Commun. 12 (2021) 6.
[16] A. Townsend, P. Rijal, J. Xiao, T.K. Tan, K.A. Huang, L. Schimanski, J. Huo, N. Gupta, R. Rahikainen, P.C. Matthews, D. Crook, S. Hoosdally, S. Dunachie, E. Barnes, T. Street, C.P. Conlon, J. Frater, C.V. Arancibia-Carcamo, J. Rudkin, N. Stoesser, F. Karpe, M. Neville, R. Ploeg, M. Oliveira, D.J. Roberts, A. A. Lamikanra, H.P. Tsang, A. Bown, R. Vipond, A.J. Mentzer, J.C. Knight, A. J. Kwok, G.R. Screaton, J. Mongkolsapaya, W. Dejnirattisai, P. Supasa, P. Klenerman, C. Dold, J.K. Baillie, S.C. Moore, P.J.M. Openshaw, M.G. Semple, L. C.W. Turtle, M. Ainsworth, A. Allcock, S. Beer, S. Bibi, D. Skelly, L. Stafford, K. Jeffrey, D. O'Donnell, E. Clutterbuck, A. Espinosa, M. Mendoza, D. Georgiou, T. Lockett, J. Martinez, E. Perez, V. Gallardo Sanchez, G. Scozzafava, A. Sobrinodiaz, H. Thraves, E. Joly, A haemagglutination test for rapid detection of antibodies to SARS-CoV-2, Nat. Commun. 12 (2021) 1951.
[17] J.D. Whitman, J. Hiatt, C.T. Mowery, B.R. Shy, R. Yu, T.N. Yamamoto, U. Rathore, G.M. Goldgof, C. Whitty, J.M. Woo, A.E. Gallman, T.E. Miller, A. G. Levine, D.N. Nguyen, S.P. Bapat, J. Balcerek, S.A. Bylsma, A.M. Lyons, S. Li, A. W. Wong, E.M. Gillis-Buck, Z.B. Steinhart, Y. Lee, R. Apathy, M.J. Lipke, J. A. Smith, T. Zheng, I.C. Boothby, E. Isaza, J. Chan, D.D. Acenas 2nd, J. Lee, T.

A. Macrae, T.S. Kyaw, D. Wu, D.L. Ng, W. Gu, V.A. York, H.A. Eskandarian, P. C. Callaway, L. Warrier, M.E. Moreno, J. Levan, L. Torres, L.A. Farrington, R. P. Loudermilk, K. Koshal, K.C. Zorn, W.F. Garcia-Beltran, D. Yang, M.G. Astudillo, B.E. Bernstein, J.A. Gelfand, E.T. Ryan, R.C. Charles, A.J. Iafrate, J.K. Lennerz, S. Miller, C.Y. Chiu, S.L. Stramer, M.R. Wilson, A. Manglik, C.J. Ye, N.J. Krogan, M.S. Anderson, J.G. Cyster, J.D. Ernst, A.H.B. Wu, K.L. Lynch, C. Bern, P.D. Hsu, A. Marson, Evaluation of SARS-CoV-2 serology assays reveals a range of test performance, Nat. Biotechnol. 38 (2020) 1174–1183.

[18] B.D. Kevadiya, J. Machhi, J. Herskovitz, M.D. Oleynikov, W.R. Blomberg, N. Bajwa, D. Soni, S. Das, M. Hasan, M. Patel, A.M. Senan, S. Gorantla, J. McMillan, B. Edagwa, R. Eisenberg, C.B. Gurumurthy, S.P.M. Reid, C. Punyadeera, L. Chang, H.E. Gendelman, Diagnostics for SARS-CoV-2 infections, Nat. Mater. 20 (2021) 593–605.

[19] I. Smyrlaki, M. Ekman, A. Lentini, N. Rufino de Sousa, N. Papanicolaou, M. Vondracek, J. Aarum, H. Safari, S. Muradrasoli, A.G. Rothfuchs, J. Albert, B. Hogberg, B. Reinius, Massive and rapid COVID-19 testing is feasible by extraction-free SARS-CoV-2 RT-PCR, Nat. Commun. 11 (2020) 4812.

[20] M.S. Han, J.-H. Byun, Y. Cho, J.H. Rim, RT-PCR for SARS-CoV-2: quantitative versus qualitative, Lancet Infect. Dis. 21 (2021) 165.

[21] N.N.Y. Tsang, H.C. So, K.Y. Ng, B.J. Cowling, G.M. Leung, D.K.M. Ip, Diagnostic performance of different sampling approaches for SARS-CoV-2 RT-PCR testing: a systematic review and meta-analysis, Lancet Infect. Dis. (2021), https://doi.org/10.1016/S1473-3099(1021)00146-00148.

[22] I. Jungreis, R. Sealfon, M. Kellis, SARS-CoV-2 gene content and COVID-19 mutation impact by comparing 44 Sarbecovirus genomes, Nat. Commun. 12 (2021) 2642.

[23] T. Koyama, D. Platt, L. Parida, Variant analysis of SARS-CoV-2 genomes, Bull. World Health Organ 98 (2020) 495–504.

[24] T. Chaibun, J. Puenpa, T. Ngamdee, N. Boonapatcharoen, P. Athamanolap, A. P. O'Mullane, S. Vongpunsawad, Y. Poovorawan, S.Y. Lee, B. Lertanantawong, Rapid electrochemical detection of coronavirus SARS-CoV-2, Nat. Commun. 12 (2021) 802.

[25] M.G. Mason, J.R. Botella, Rapid (30-second), equipment-free purification of nucleic acids using easy-to-make dipsticks, Nat. Protoc. 15 (2020) 3663–3677.

[26] Z. Zhang, Q. Bi, S. Fang, L. Wei, X. Wang, J. He, Y. Wu, X. Liu, W. Gao, R. Zhang, W. Gong, Q. Su, A.S. Azman, J. Lessler, X. Zou, Insight into the practical performance of RT-PCR testing for SARS-CoV-2 using serological data: a cohort study, Lancet Microbe 2 (2021) e79–e87.

[27] M.P. Coryell, M. Iakiviak, N. Pereira, P.P. Murugkar, J. Rippe, D.B. Williams, T. Heald-Sargent, L.N. Sanchez-Pinto, J. Chavez, J.L. Hastie, R.L. Sava, C.Z. Lien, T.T. Wang, W.J. Muller, M.A. Fischbach, P.E. Carlson, A method for detection of SARS-CoV-2 RNA in healthy human stool: a validation study, Lancet Microbe 2 (2021) e259–e266.

[28] H.C. Zhen Zhao, Wenxing Song, Xiaoling Ru, Wenhua Zhou, Xuefeng Yu, A simple magnetic nanoparticles-based viral RNA extraction method for efficient detection of SARS-CoV-2, BioRxiv (2020), https://doi.org/10.1101/2020.1102.1122.961268.

[29] J.E. Celis, W. Espejo, E. Paredes-Osses, S.A. Contreras, G. Chiang, P. Bahamonde, Plastic residues produced with confirmatory testing for COVID-19: Classification, quantification, fate, and impacts on human health, Sci. Total Environ. 760 (2021), 144167.

[30] J.S. Bloom, L. Sathe, C. Munugala, E.M. Jones, M. Gasperini, N.B. Lubock, F. Yarza, E.M. Thompson, K.M. Kovary, J. Park, D. Marquette, S. Kay, M. Lucas, T. Love, A. Sina Booeshaghi, O.F. Brandenberg, L. Guo, J. Boocock, M. Hochman, S.W. Simpkins, I. Lin, N. LaPierre, D. Hong, Y. Zhang, G. Oland, B.J. Choe, S. Chandrasekaran, E.E. Hilt, M.J. Butte, R. Damoiseaux, C. Kravit, A.R. Cooper, Y. Yin, L. Pachter, O.B. Garner, J. Flint, E. Eskin, C. Luo, S. Kosuri, L. Kruglyak, V. A. Arboleda, Massively scaled-up testing for SARS-CoV-2 RNA via next-generation sequencing of pooled and barcoded nasal and saliva samples, Nat. Biomed. Eng. 5 (2021) 657–665.

[31] S. Lohse, T. Pfuhl, B. Berkó-Göttel, J. Rissland, T. Geißler, B. Gärtner, S.L. Becker, S. Schneitler, S. Smola, Pooling of samples for testing for SARS-CoV-2 in asymptomatic people, Lancet Infect. Dis. 20 (2020) 1231–1232.

[32] M. Plebani, Persistent viral RNA shedding in COVID-19: Caution, not fear, EBioMedicine 64 (2021), 103234.

[33] O. Vandenberg, D. Martiny, O. Rochas, A. van Belkum, Z. Kozlakidis, Considerations for diagnostic COVID-19 tests, Nat. Rev. Microbiol 19 (2021) 171–183.

[34] N.P. Steven Woloshin, Aaron S. Kesselheim, False negative tests for SARS-CoV-2 infection — challenges and implications, N. Engl. J. Med. 383 (2020), e38.

[35] S. Contreras, J. Dehning, M. Loidolt, J. Zierenberg, F.P. Spitzner, J.H. Urrea-Quintero, S.B. Mohr, M. Wilczek, M. Wibral, V. Priesemann, The challenges of containing SARS-CoV-2 via test-trace-and-isolate, Nat. Commun. 12 (2021) 378.

[36] M. Morvaridzadeh, E. Sadeghi, S. Agah, S.M. Nachvak, S. Fazelian, F. Moradi, E. Persad, J. Heshmati, Effect of melatonin supplementation on oxidative stress parameters: a systematic review and meta-analysis, Pharm. Res. 161 (2020), 105210.

[37] J.N. Kanji, N. Zelyas, C. MacDonald, K. Pabbaraju, M.N. Khan, A. Prasad, J. Hu, M. Diggle, B.M. Berenger, G. Tipples, False negative rate of COVID-19 PCR testing: a discordant testing analysis, Virol. J. 18 (2021) 13.

[38] M. Kanamoto, M. Tobe, T. Takazawa, S. Saito, COVID-19 with repeated positive test results for SARS-CoV-2 by PCR and then negative test results twice during intensive care: a case report, J. Med. Case Rep. 14 (2020) 191.

[39] T. Beduk, D. Beduk, J.I. de Oliveira Filho, F. Zihnioglu, C. Cicek, R. Sertoz, B. Arda, T. Goksel, K. Turhan, K.N. Salama, S. Timur, Rapid point-of-care COVID-19 diagnosis with a gold-nanoarchitecture-assisted laser-scribed graphene biosensor, Anal. Chem. 93 (2021) 8585–8594.

[40] M.R. Willner, P.J. Vikesland, Nanomaterial enabled sensors for environmental contaminants, J. Nanobiotechnology 16 (2018) 95.

[41] F. Zhang, Z. Wang, M.G. Vijver, W. Peijnenburg, Probing nano-QSAR to assess the interactions between carbon nanoparticles and a SARS-CoV-2 RNA fragment, Ecotoxicol. Environ. Saf. 219 (2021), 112357.

[42] M. Alafeef, P. Moitra, K. Dighe, D. Pan, RNA-extraction-free nano-amplified colorimetric test for point-of-care clinical diagnosis of COVID-19, Nat. Protoc. 16 (2021) 3141–3162.

[43] L. Wang, X. Wang, Y. Wu, M. Guo, C. Gu, C. Dai, D. Kong, Y. Wang, C. Zhang, D. Qu, C. Fan, Y. Xie, Z. Zhu, Y. Liu, D. Wei, Rapid and ultrasensitive electromechanical detection of ions, biomolecules and SARS-CoV-2 RNA in unamplified samples, Nat. Biomed. Eng. (2022), https://doi.org/10.1038/s41551-41021-00833-41557.

[44] S.K. Elledge, X.X. Zhou, J.R. Byrnes, A.J. Martinko, I. Lui, K. Pance, S.A. Lim, J. E. Glasgow, A.A. Glasgow, K. Turcios, N.S. Iyer, L. Torres, M.J. Peluso, T. J. Henrich, T.T. Wang, C.M. Tato, K.K. Leung, B. Greenhouse, J.A. Wells, Engineering luminescent biosensors for point-of-care SARS-CoV-2 antibody detection, Nat. Biotechnol. (2021), https://doi.org/10.1038/s41587-41021-00878-41588.

[45] D. Li, H. Chen, X. Gao, X. Mei, L. Yang, Development of general methods for detection of virus by engineering fluorescent silver nanoclusters, ACS Sens 6 (2021) 613–627.

[46] A. Stambaugh, J.W. Parks, M.A. Stott, G.G. Meena, A.R. Hawkins, H. Schmidt, Optofluidic multiplex detection of single SARS-CoV-2 and influenza A antigens using a novel bright fluorescent probe assay, Proc. Natl. Acad. Sci. USA 118 (2021) e2103480118.

[47] Y. Rivenson, H. Wang, Z. Wei, K. de Haan, Y. Zhang, Y. Wu, H. Gunaydin, J. E. Zuckerman, T. Chong, A.E. Sisk, L.M. Westbrook, W.D. Wallace, A. Ozcan, Virtual histological staining of unlabelled tissue-autofluorescence images via deep learning, Nat. Biomed. Eng. 3 (2019) 466–477.

[48] S. Zhou, D. Tu, Y. Liu, W. You, Y. Zhang, W. Zheng, X. Chen, Ultrasensitive point-of-care test for tumor marker in human saliva based on luminescence-amplification strategy of lanthanide nanoprobes, Adv. Sci. 8 (2021), 2002657.

[49] D.M. Shcherbakova, M. Baloban, A.V. Emelyanov, M. Brenowitz, P. Guo, V. V. Verkhusha, Bright monomeric near-infrared fluorescent proteins as tags and biosensors for multiscale imaging, Nat. Commun. 7 (2016) 12405.

[50] M. Zhao, B. Li, H. Zhang, F. Zhang, Activatable fluorescence sensors for in vivo bio-detection in the second near-infrared window, Chem. Sci. 12 (2020) 3448–3459.

[51] Y. Cai, Z. Wei, C. Song, C. Tang, W. Han, X. Dong, Optical nano-agents in the second near-infrared window for biomedical applications, Chem. Soc. Rev. 48 (2019) 22–37.

[52] M.E. Matlashov, D.M. Shcherbakova, J. Alvelid, M. Baloban, F. Pennacchietti, A. A. Shemetov, I. Testa, V.V. Verkhusha, A set of monomeric near-infrared fluorescent proteins for multicolor imaging across scales, Nat. Commun. 11 (2020) 239.

[53] R. Marin, A. Benayas, N. García-Carillo, J. Lifante, J. Yao, D. Mendez-Gonzalez, F. Sanz-Rodríguez, J. Rubio-Retama, L.V. Besteiro, D. Jaque, Nanoprobes for biomedical imaging with tunable near-infrared optical properties obtained via green, Synth., Ad Photonics Res. 3 (2021).

[54] K.B. Bec, J. Grabska, C.W. Huck, Principles and applications of miniaturized near-infrared (NIR) spectrometers, Chemistry 27 (2021) 1514–1532.

[55] R. Nissler, O. Bader, M. Dohmen, S.G. Walter, C. Noll, G. Selvaggio, U. Gross, S. Kruss, Remote near infrared identification of pathogens with multiplexed nanosensors, Nat. Commun. 11 (2020) 5995.

[56] M. Dinarvand, E. Neubert, D. Meyer, G. Selvaggio, F.A. Mann, L. Erpenbeck, S. Kruss, Near-infrared imaging of serotonin release from cells with fluorescent nanosensors, Nano Lett. 19 (2019) 6604–6611.

[57] H. Wu, R. Nissler, V. Morris, N. Herrmann, P. Hu, S.J. Jeon, S. Kruss, J.P. Giraldo, Monitoring plant health with near-infrared fluorescent H2O2 nanosensors, Nano Lett. 20 (2020) 2432–2442.

[58] S.Y. Cho, X. Gong, V.B. Koman, M. Kuehne, S.J. Moon, M. Son, T.T.S. Lew, P. Gordiichuk, X. Jin, H.D. Sikes, M.S. Strano, Cellular lensing and near infrared fluorescent nanosensor arrays to enable chemical efflux cytometry, Nat. Commun. 12 (2021) 3079.

[59] D.P. Salem, X. Gong, A.T. Liu, K. Akombi, M.S. Strano, Immobilization and function of nIR-fluorescent carbon nanotube sensors on paper substrates for fluidic manipulation, Anal. Chem. 92 (2020) 916–923.

[60] G. Selvaggio, A. Chizhik, R. Nissler, L. Kuhlemann, D. Meyer, L. Vuong, H. Preiss, N. Herrmann, F.A. Mann, Z. Lv, T.A. Oswald, A. Spreinat, L. Erpenbeck, J. Grosshans, V. Karius, A. Janshoff, J. Pablo Giraldo, S. Kruss, Exfoliated near infrared fluorescent silicate nanosheets for (bio)photonics, Nat. Commun. 11 (2020) 1495.

[61] Y. Shu, J. Yan, Q. Lu, Z. Ji, D. Jin, Q. Xu, X. Hu, Pb ions enhanced fluorescence of Ag2S QDs with tunable emission in the NIR-II window: Facile one pot synthesis and their application in NIR-II fluorescent bio-sensing, Sens. Actuators B: Chem. 307 (2020), 127593.

[62] S. Liu, H. Ou, Y. Li, H. Zhang, J. Liu, X. Lu, R.T.K. Kwok, J.W.Y. Lam, D. Ding, B. Z. Tang, Planar and twisted molecular structure leads to the high brightness of semiconducting polymer nanoparticles for NIR-IIa fluorescence imaging, J. Am. Chem. Soc. 142 (2020) 15146–15156.

[63] Q.D. Mac, D.V. Mathews, J.A. Kahla, C.M. Stoffers, O.M. Delmas, B.A. Holt, A. B. Adams, G.A. Kwong, Non-invasive early detection of acute transplant rejection via nanosensors of granzyme B activity, Nat. Biomed. Eng. 3 (2019) 281–291.

[64] X. Xiao, T. Wu, J. Cao, C. Zhu, Y. Liu, X. Zhang, Y. Shen, Rational engineering of chromic material as near-infrared ratiometric fluorescent nanosensor for H_2S monitoring in real food samples, Sens. Actuators B: Chem. 323 (2020), 128707.

[65] M. Zhao, B. Li, Y. Wu, H. He, X. Zhu, H. Zhang, C. Dou, L. Feng, Y. Fan, F. Zhang, A tumor-microenvironment-responsive lanthanide-cyanine FRET sensor for NIR-II luminescence-lifetime in situ imaging of hepatocellular carcinoma, Adv. Mater. 32 (2020), 2001172.

[66] V. Pansare, S. Hejazi, W. Faenza, R.K. Prud'homme, Review of long-wavelength optical and NIR imaging materials: contrast agents, fluorophores and multifunctional nano carriers, Chem. Mater. 24 (2012) 812–827.

[67] B. Li, Y. Hu, Z. Shen, Z. Ji, L. Yao, S. Zhang, Y. Zou, D. Tang, Y. Qing, S. Wang, G. Zhao, X. Wang, Photocatalysis driven by near-infrared light: materials design and engineering for environmentally friendly photoreactions, ACS EST Eng. 1 (2021) 947–964.

[68] N. Sethuraman, S.S. Jeremiah, A. Ryo, Interpreting diagnostic tests for SARS-CoV-2, JAMA 323 (2020) 2249–2251.

[69] P. Moitra, M. Alafeef, K. Dighe, M.B. Frieman, D. Pan, Selective naked-eye detection of SARS-CoV-2 mediated by N gene targeted antisense oligonucleotide capped plasmonic nanoparticles, ACS Nano 14 (2020) 7617–7627.

[70] X. Yin, C. Zhang, Y. Guo, Y. Yang, Y. Xing, W. Que, PbS QD-based photodetectors: future-oriented near-infrared detection technology, J. Mater. Chem. C. 9 (2021) 417–438.

[71] M. Zhang, J. Yue, R. Cui, Z. Ma, H. Wan, F. Wang, S. Zhu, Y. Zhou, Y. Kuang, Y. Zhong, D.W. Pang, H. Dai, Bright quantum dots emitting at approximately 1,600 nm in the NIR-IIb window for deep tissue fluorescence imaging, Proc. Natl. Acad. Sci. USA 115 (2018) 6590–6595.

[72] P. Moitra, M. Alafeef, K. Dighe, Z. Sheffield, D. Dahal, D. Pan, Synthesis and characterisation of N-gene targeted NIR-II fluorescent probe for selective localisation of SARS-CoV-2, Chem. Commun. 57 (2021) 6229–6232.

[73] G. Seo, G. Lee, M.J. Kim, S.H. Baek, M. Choi, K.B. Ku, C.S. Lee, S. Jun, D. Park, H. G. Kim, S.J. Kim, J.O. Lee, B.T. Kim, E.C. Park, S.I. Kim, Rapid detection of COVID-19 causative virus (SARS-CoV-2) in human nasopharyngeal swab specimens using field-effect transistor-based biosensor, ACS Nano 14 (2020) 5135–5142.

[74] H. Zhang, J.M. Penninger, Y. Li, N. Zhong, A.S. Slutsky, Angiotensin-converting enzyme 2 (ACE2) as a SARS-CoV-2 receptor: molecular mechanisms and potential therapeutic target, Intensive Care Med. 46 (2020) 586–590.

[75] J. Lan, J. Ge, J. Yu, S. Shan, H. Zhou, S. Fan, Q. Zhang, X. Shi, Q. Wang, L. Zhang, X. Wang, Structure of the SARS-CoV-2 spike receptor-binding domain bound to the ACE2 receptor, Nature 581 (2020) 215–220.

[76] R.L. Pinals, F. Ledesma, D. Yang, N. Navarro, S. Jeong, J.E. Pak, L. Kuo, Y. C. Chuang, Y.W. Cheng, H.Y. Sun, M.P. Landry, Rapid SARS-CoV-2 spike protein detection by carbon nanotube-based near-infrared nanosensors, Nano Lett. 21 (2021) 2272–2280.

[77] A. Graf, L. Tropf, Y. Zakharko, J. Zaumseil, M.C. Gather, Near-infrared exciton-polaritons in strongly coupled single-walled carbon nanotube microcavities, Nat. Commun. 7 (2016) 13078.

[78] T. Jiang, C.A. Amadei, N. Gou, Y. Lin, J. Lan, C.D. Vecitis, A.Z. Gu, Toxicity of single-walled carbon nanotubes (SWCNTs): effect of lengths, functional groups and electronic structures revealed by a quantitative toxicogenomics assay, Environ. Sci. Nano 7 (2020) 1348–1364.

[79] N. Hadrup, K.B. Knudsen, M. Carriere, M. Mayne-L'Hermite, L. Bobyk, S. Allard, F. Miserque, B. Pibaleau, M. Pinault, H. Wallin, U. Vogel, Safe-by-design strategies for lowering the genotoxicity and pulmonary inflammation of multiwalled carbon nanotubes: reduction of length and the introduction of COOH groups, Environ. Toxicol. Pharm. 87 (2021), 103702.

[80] J. Lin, Y. Jiang, Y. Luo, H. Guo, C. Huang, J. Peng, Y. Cao, Multi-walled carbon nanotubes (MWCNTs) transformed THP-1 macrophages into foam cells: impact of pulmonary surfactant component dipalmitoylphosphatidylcholine, J. Hazard Mater. 392 (2020), 122286.

[81] Y.X. Sham Nambulli, Natasha L. Tilston-Lunel, Linda J. Rennick, Zhe Sang, William B. Klimstra, Douglas S. Reed, Nicholas A. Crossland, Yi Shi, W. Paul Duprex, Inhalable nanobody (PiN-21) prevents and treats SARS-CoV-2 infections in Syrian hamsters at ultra-low doses, Sci. Adv. 7 (2021) eabh0319.

[82] K. Guo, S. Wustoni, A. Koklu, E. Diaz-Galicia, M. Moser, A. Hama, A.A. Alqahtani, A.N. Ahmad, F.S. Alhamlan, M. Shuaib, A. Pain, I. McCulloch, S.T. Arold, R. Grunberg, S. Inal, Rapid single-molecule detection of COVID-19 and MERS antigens via nanobody-functionalized organic electrochemical transistors, Nat. Biomed. Eng. 5 (2021) 666–677.

[83] G. Yang, Z. Li, I. Mohammed, L. Zhao, W. Wei, H. Xiao, W. Guo, Y. Zhao, F. Qu, Y. Huang, Identification of SARS-CoV-2-against aptamer with high neutralization activity by blocking the RBD domain of spike protein 1, Signal Transduct. Target Ther. 6 (2021) 227.

[84] Z. Chen, Q. Wu, J. Chen, X. Ni, J. Dai, A DNA aptamer based method for detection of SARS-CoV-2 nucleocapsid protein, Virol. Sin. 35 (2020) 351–354.

[85] Y. Song, J. Song, X. Wei, M. Huang, M. Sun, L. Zhu, B. Lin, H. Shen, Z. Zhu, C. Yang, Discovery of aptamers targeting the receptor-binding domain of the SARS-CoV-2 spike glycoprotein, Anal. Chem. 92 (2020) 9895–9900.

[86] N. Kacherovsky, L.F. Yang, H.V. Dang, E.L. Cheng, I.I. Cardle, A.C. Walls, M. McCallum, D.L. Sellers, F. DiMaio, S.J. Salipante, D. Corti, D. Veesler, S. H. Pun, Discovery and characterization of spike N-terminal domain-binding aptamers for rapid SARS-CoV-2 detection, Angew. Chem. Int Ed. Engl. (2021), https://doi.org/10.1002/anie.202107730.

[87] J. Li, Z. Zhang, J. Gu, H.D. Stacey, J.C. Ang, A. Capretta, C.D.M. Filipe, K. L. Mossman, C. Balion, B.J. Salena, D. Yamamura, L. Soleymani, M.S. Miller, J. D. Brennan, Y. Li, Diverse high-affinity DNA aptamers for wild-type and B.1.1.7 SARS-CoV-2 spike proteins from a pre-structured DNA library, Nucleic Acids Res 49 (2021) 7267–7279.

[88] J.H. Lee, M. Choi, Y. Jung, S.K. Lee, C.S. Lee, J. Kim, J. Kim, N.H. Kim, B.T. Kim, H.G. Kim, A novel rapid detection for SARS-CoV-2 spike 1 antigens using human angiotensin converting enzyme 2 (ACE2), Biosens. Bioelectron. 171 (2021), 112715.

[89] S.Y. Cho, X. Jin, X. Gong, S. Yang, J. Cui, M.S. Strano, Antibody-free rapid detection of SARS-CoV-2 proteins using corona phase molecular recognition to accelerate development time, Anal. Chem. 93 (2021) 14685–14693.

[90] Q.X. Long, B.Z. Liu, H.J. Deng, G.C. Wu, K. Deng, Y.K. Chen, P. Liao, J.F. Qiu, Y. Lin, X.F. Cai, D.Q. Wang, Y. Hu, J.H. Ren, N. Tang, Y.Y. Xu, L.H. Yu, Z. Mo, F. Gong, X.L. Zhang, W.G. Tian, L. Hu, X.X. Zhang, J.L. Xiang, H.X. Du, H.W. Liu, C.H. Lang, X.H. Luo, S.B. Wu, X.P. Cui, Z. Zhou, M.M. Zhu, J. Wang, C.J. Xue, X. F. Li, L. Wang, Z.J. Li, K. Wang, C.C. Niu, Q.J. Yang, X.J. Tang, Y. Zhang, X.M. Liu, J.J. Li, D.C. Zhang, F. Zhang, P. Liu, J. Yuan, Q. Li, J.L. Hu, J. Chen, A.L. Huang, Antibody responses to SARS-CoV-2 in patients with COVID-19, Nat. Med. 26 (2020) 845–848.

[91] C. Gaebler, Z. Wang, J.C.C. Lorenzi, F. Muecksch, S. Finkin, M. Tokuyama, A. Cho, M. Jankovic, D. Schaefer-Babajew, T.Y. Oliveira, M. Cipolla, C. Viant, C. O. Barnes, Y. Bram, G. Breton, T. Hagglof, P. Mendoza, A. Hurley, M. Turroja, K. Gordon, K.G. Millard, V. Ramos, F. Schmidt, Y. Weisblum, D. Jha, M. Tankelevich, G. Martinez-Delgado, J. Yee, R. Patel, J. Dizon, C. Unson-O'Brien, I. Shimeliovich, D.F. Robbiani, Z. Zhao, A. Gazumyan, R.E. Schwartz, T. Hatziioannou, P.J. Bjorkman, S. Mehandru, P.D. Bieniasz, M. Caskey, M. C. Nussenzweig, Evolution of antibody immunity to SARS-CoV-2, Nature 591 (2021) 639–644.

[92] D.F. Cruz, C.M. Fontes, D. Semeniak, J. Huang, A. Hucknall, A. Chilkoti, M. H. Mikkelsen, Ultrabright fluorescence readout of an inkjet-printed immunoassay using plasmonic nanogap cavities, Nano Lett. 20 (2020) 4330–4336.

[93] T. Liu, J. Hsiung, S. Zhao, J. Kost, D. Sreedhar, C.V. Hanson, K. Olson, D. Keare, S. T. Chang, K.P. Bliden, P.A. Gurbel, U.S. Tantry, J. Roche, C. Press, J. Boggs, J. P. Rodriguez-Soto, J.G. Montoya, M. Tang, H. Dai, Quantification of antibody avidities and accurate detection of SARS-CoV-2 antibodies in serum and saliva on plasmonic substrates, Nat. Biomed. Eng. 4 (2020) 1188–1196.

[94] J. Li, Y. Liu, Y. Xu, L. Li, Y. Sun, W. Huang, Recent advances in the development of NIR-II organic emitters for biomedicine, Coord. Chem. Rev. 415 (2020), 213318.

[95] W. Xu, D. Wang, B.Z. Tang, NIR-II AIEgens: a win-win integration towards bioapplications, Angew. Chem. Int Ed. Engl. 60 (2021) 7476–7487.

[96] F. Ye, Y. Liu, J. Chen, S.H. Liu, W. Zhao, J. Yin, Tetraphenylene-coated near-infrared benzoselenodiazole dye: AIE behavior, mechanochromism, and bioimaging, Org. Lett. 21 (2019) 7213–7217.

[97] P. Fozouni, S. Son, M. Diaz de Leon Derby, G.J. Knott, C.N. Gray, M. V. D'Ambrosio, C. Zhao, N.A. Switz, G.R. Kumar, S.I. Stephens, D. Boehm, C. L. Tsou, J. Shu, A. Bhuiya, M. Armstrong, A.R. Harris, P.Y. Chen, J.M. Osterloh, A. Meyer-Franke, B. Joehnk, K. Walcott, A. Sil, C. Langelier, K.S. Pollard, E. D. Crawford, A.S. Puschnik, M. Phelps, A. Kistler, J.L. DeRisi, J.A. Doudna, D. A. Fletcher, M. Ott, Amplification-free detection of SARS-CoV-2 with CRISPR-Cas13a and mobile phone microscopy, Cell 184 (2021) 323–333 e329.

[98] R. Chen, C. Ren, M. Liu, X. Ge, M. Qu, X. Zhou, M. Liang, Y. Liu, F. Li, Early detection of SARS-CoV-2 seroconversion in humans with aggregation-induced near-infrared emission nanoparticle-labeled lateral flow immunoassay, ACS Nano 15 (2021) 8996–9004.

[99] S. Ye, N. Hananya, O. Green, H. Chen, A.Q. Zhao, J. Shen, D. Shabat, D. Yang, A highly selective and sensitive chemiluminescent probe for real-time monitoring of hydrogen peroxide in cells and animals, Angew. Chem. Int Ed. Engl. 59 (2020) 14326–14330.

[100] S. Patchett, Z. Lv, W. Rut, M. Bekes, M. Drag, S.K. Olsen, T.T. Huang, A molecular sensor determines the ubiquitin substrate specificity of SARS-CoV-2 papain-like protease, Cell Rep. 36 (2021), 109754.

[101] Z.Z. Si Si Liew, Penghui Cheng, Shasha He, Chi Zhang, Kanyi Pu, Renal-clearable molecular probe for near-infrared fluorescence imaging and urinalysis of SARS-CoV-2, J. Am. Chem. Soc. (2021), https://doi.org/10.1021/jacs.1021c08017.

[102] R. Gozalbo-Rovira, E. Gimenez, V. Latorre, C. Frances-Gomez, E. Albert, J. Buesa, A. Marina, M.L. Blasco, J. Signes-Costa, J. Rodriguez-Diaz, R. Geller, D. Navarro, SARS-CoV-2 antibodies, serum inflammatory biomarkers and clinical severity of hospitalized COVID-19 patients, J. Clin. Virol. 131 (2020), 104611.

[103] M. Garg, A.L. Sharma, S. Singh, Advancement in biosensors for inflammatory biomarkers of SARS-CoV-2 during 2019-2020, Biosens. Bioelectron. 171 (2021), 112703.

[104] L. Zhang, H. Guo, Biomarkers of COVID-19 and technologies to combat SARS-CoV-2, Adv. Biomark. Sci. Technol. 2 (2020) 1–23.

[105] J. Guo, S. Chen, S. Tian, K. Liu, J. Ni, M. Zhao, Y. Kang, X. Ma, J. Guo, 5G-enabled ultra-sensitive fluorescence sensor for proactive prognosis of COVID-19, Biosens. Bioelectron. 181 (2021), 113160.

[106] C.T. Jackson, S. Jeong, G.F. Dorlhiac, M.P. Landry, Advances in engineering near-infrared luminescent materials, iScience 24 (2021), 102156.

[107] S. Diao, J.L. Blackburn, G. Hong, A.L. Antaris, J. Chang, J.Z. Wu, B. Zhang, K. Cheng, C.J. Kuo, H. Dai, Fluorescence imaging in vivo at wavelengths beyond 1500 nm, Angew. Chem. Int Ed. Engl. 54 (2015) 14758–14762.

[108] M.M.D. Alexander Spreinat, Jan Lüttgens, Niklas Herrmann, Lars F. Klepzig, Robert Nißler, Sabrina Weber, Florian A. Mann, Jannika Lauth, Sebastian Kruss, Quantum defects in fluorescent carbon nanotubes for sensing and mechanistic, Stud., chemRxiv (2021), https://doi.org/10.26434/chemrxiv.14647527.v14647521.

[109] Y. Zhong, Z. Ma, S. Zhu, J. Yue, M. Zhang, A.L. Antaris, J. Yuan, R. Cui, H. Wan, Y. Zhou, W. Wang, N.F. Huang, J. Luo, Z. Hu, H. Dai, Boosting the down-shifting luminescence of rare-earth nanocrystals for biological imaging beyond 1500 nm, Nat. Commun. 8 (2017) 737.
[110] D. Li, S. He, Y. Wu, J. Liu, Q. Liu, B. Chang, Q. Zhang, Z. Xiang, Y. Yuan, C. Jian, A. Yu, Z. Cheng, Excretable lanthanide nanoparticle for biomedical imaging and surgical navigation in the second near-infrared window, Adv. Sci. 6 (2019), 1902042.
[111] J. Shi, X. Sun, S. Zheng, J. Li, X. Fu, H. Zhang, A new near-infrared persistent luminescence nanoparticle as a multifunctional nanoplatform for multimodal imaging and cancer therapy, Biomaterials 152 (2018) 15–23.
[112] C. Wang, M. Niu, W. Wang, L. Su, H. Feng, H. Lin, X. Ge, R. Wu, Q. Li, J. Liu, H. Yang, J. Song, In situ activatable ratiometric NIR-II fluorescence nanoprobe for quantitative detection of H2S in colon cancer, Anal. Chem. 93 (2021) 9356–9363.
[113] Y. Fan, P. Wang, Y. Lu, R. Wang, L. Zhou, X. Zheng, X. Li, J.A. Piper, F. Zhang, Lifetime-engineered NIR-II nanoparticles unlock multiplexed in vivo imaging, Nat. Nanotechnol. 13 (2018) 941–946.
[114] X. Li, M. Jiang, Y. Li, Z. Xue, S. Zeng, H. Liu, 808nm laser-triggered NIR-II emissive rare-earth nanoprobes for small tumor detection and blood vessel imaging, Mater. Sci. Eng. C. Mater. Biol. Appl. 100 (2019) 260–268.
[115] J. Kim, J.H. Kwon, J. Jang, H. Lee, S. Kim, Y.K. Hahn, S.K. Kim, K.H. Lee, S. Lee, H. Pyo, C.S. Song, J. Lee, Rapid and background-free detection of avian influenza virus in opaque sample using NIR-to-NIR upconversion nanoparticle-based lateral flow immunoassay platform, Biosens. Bioelectron. 112 (2018) 209–215.
[116] Y. Zhai, X. Yang, F. Wang, Z. Li, G. Ding, Z. Qiu, Y. Wang, Y. Zhou, S.T. Han, Infrared-sensitive memory based on direct-grown MoS2 -upconversion-nanoparticle heterostructure, Adv. Mater. 30 (2018), 1803563.
[117] D. Kang, S. Lee, H. Shin, J. Pyun, J. Lee, An efficient NIR-to-NIR signal-based LRET system for homogeneous competitive immunoassay, Biosens. Bioelectron. 150 (2020), 111921.
[118] P. Zhu, S. Gao, H. Lin, X. Lu, B. Yang, L. Zhang, Y. Chen, J. Shi, Inorganic nanoshell-stabilized liquid metal for targeted photonanomedicine in NIR-II biowindow, Nano Lett. 19 (2019) 2128–2137.
[119] Z. Cao, L. Feng, G. Zhang, J. Wang, S. Shen, D. Li, X. Yang, Semiconducting polymer-based nanoparticles with strong absorbance in NIR-II window for in vivo photothermal therapy and photoacoustic imaging, Biomaterials 155 (2018) 103–111.
[120] D. Franke, D.K. Harris, O. Chen, O.T. Bruns, J.A. Carr, M.W.B. Wilson, M. G. Bawendi, Continuous injection synthesis of indium arsenide quantum dots emissive in the short-wavelength infrared, Nat. Commun. 7 (2016) 12749.
[121] H. Ding, X.-X. Zhou, J.-S. Wei, X.-B. Li, B.-T. Qin, X.-B. Chen, H.-M. Xiong, Carbon dots with red/near-infrared emissions and their intrinsic merits for biomedical applications, Carbon 167 (2020) 322–344.
[122] D. Li, Q. Liu, Q. Qi, H. Shi, E.C. Hsu, W. Chen, W. Yuan, Y. Wu, S. Lin, Y. Zeng, Z. Xiao, L. Xu, Y. Zhang, T. Stoyanova, W. Jia, Z. Cheng, Gold nanoclusters for NIR-II fluorescence imaging of bones, Small 16 (2020), 2003851.
[123] X. Song, W. Zhu, X. Ge, R. Li, S. Li, X. Chen, J. Song, J. Xie, X. Chen, H. Yang, A. New, Class of NIR-II gold nanocluster-based protein biolabels for in vivo tumor-targeted imaging, Angew. Chem. Int Ed. Engl. 60 (2021) 1306–1312.
[124] Y. Li, Z. Cai, S. Liu, H. Zhang, S.T.H. Wong, J.W.Y. Lam, R.T.K. Kwok, J. Qian, B. Z. Tang, Design of AIEgens for near-infrared IIb imaging through structural modulation at molecular and morphological levels, Nat. Commun. 11 (2020) 1255.
[125] I. Chowdhury, M.C. Duch, C.C. Gits, M.C. Hersam, S.L. Walker, Impact of synthesis methods on the transport of single walled carbon nanotubes in the aquatic environment, Environ. Sci. Technol. 46 (2012) 11752–11760.
[126] Y. Yomogida, T. Tanaka, M. Tsuzuki, X. Wei, H. Kataura, Automatic sorting of single-chirality single-wall carbon nanotubes using hydrophobic cholates: implications for multicolor near-infrared optical technologies, ACS Appl. Nano Mater. 3 (2020) 11289–11297.
[127] D. Li, Z. Chen, X. Mei, Fluorescence enhancement for noble metal nanoclusters, Adv. Colloid Interface Sci. 250 (2017) 25–39.
[128] Y. Li, G. Bai, S. Zeng, J. Hao, Theranostic carbon dots with innovative NIR-II emission for in vivo renal-excreted optical imaging and photothermal therapy, ACS Appl. Mater. Interfaces 11 (2019) 4737–4744.
[129] Z. Wang, L. Yu, Y. Wang, C. Wang, Q. Mu, X. Liu, M. Yu, Dynamic adjust of non-radiative and radiative attenuation of AIE molecules reinforces NIR-II imaging mediated photothermal therapy and immunotherapy, Adv. SCi. (2022), https://doi.org/10.1002/advs.202104793.
[130] Q. Zhang, P. Yu, Y. Fan, C. Sun, H. He, X. Liu, L. Lu, M. Zhao, H. Zhang, F. Zhang, Bright and stable NIR-II J-aggregated AIE dibodipy-based fluorescent probe for dynamic in vivo bioimaging, Angew. Chem. Int Ed. Engl. 60 (2021) 3967–3973.
[131] H. Wang, Z. Peng, Y. Long, H. Chen, Y. Yang, N. Li, F. Liu, A simple and reusable fluorescent sensor for heme proteins based on a conjugated polymer-doped electrospun nanofibrous membrane, Talanta 94 (2012) 216–222.
[132] J. Zhang, X. Li, J.-C. Zhang, J.-S. Yan, H. Zhu, J.-J. Liu, R. Li, S. Ramakrishna, Y.-Z. Long, Ultrasensitive and reusable upconversion-luminescence nanofibrous indicator paper for in-situ dual detection of single droplet, Chem. Eng. J. 382 (2020), 122779.
[133] V. Shumeiko, E. Malach, Y. Helman, Y. Paltiel, G. Bisker, Z. Hayouka, O. Shoseyov, A nanoscale optical biosensor based on peptide encapsulated SWCNTs for detection of acetic acid in the gaseous phase, Sens. Actuators B: Chem. 327 (2021), 128832.

Dan Li worked for biosensing research in the Department of Chemistry at the University of Massachusetts, Amherst under the supervision of Professor Vincent M. Rotello from December 2018 to December 2019. She is an Associate Professor at Jinzhou Medical University. Her current research focuses on the synthesis and application of nanoclusters for biomedical diagnosis.

Zipeng Zhou has joined the first affiliated hospital of Jinzhou University as a PhD candidate under the guidance of Prof. Xifan Mei. The focus of his research is the development of nanomaterials for diagnosis and therapy applications.

Jiachen Sun has joined the first affiliated hospital of Jinzhou University for a Master's Degree under the guidance of Prof. Xifan Mei. The focus of his research is the development of nanomaterials for diagnosis and therapy applications.

Xifan Mei is a distinguished professor of the spine Department of the First Affiliated Hospital of Jinzhou Medical University. He is also the chairman designate of the trauma branch of the Liaoning Medical Association, vice chairman of the Council of the Liaoning society of neuroscience. His current research focuses on the application of nanomaterials for biomedical science.